MODES OF OBLIQUE COMPRESSION: LATE CENOZOIC TECTONICS OF THE SOUTH ISLAND OF NEW ZEALAND

R. I. Walcott
School of Earth Sciences
Victoria University of Wellington
Wellington, New Zealand

Abstract. When continental crust is consumed at a plate boundary, it is not subducted into the asthenosphere like oceanic crust but either is pushed up and eroded or is moved sideways away from the collision to spread the deformation over adjacent and in some cases, far distant, regions. Both modes occur in the South Island of New Zealand, where the Australian and Pacific plates move obliquely relative to each other so that there is motion both parallel and perpendicular to the plate boundary. The perpendicular component has resulted in the rise and erosion of the Southern Alps. Because compression is continuing, the early stages of continental collision can be studied in one of the most simple and accessible of plate boundaries. Since 6.4 Ma, 90 km of shortening in the continental crust of the central South Island has occurred (somewhat less in the south and more in the north), together with 230 km of dextral strike-slip. Prior to 6.4 Ma, relative plate motion was strike-slip with only a small compressive component. Hence a strip of continental lithosphere some 90 km wide has been consumed in Pliocene–Quaternary time. It has been accommodated in different ways in different parts of the plate boundary. In the south, that part of the Pliocene–Quaternary convergence not involved in subduction of oceanic lithosphere of the Australian plate under Fiordland is accommodated by low-intensity deformation distributed up to 200 km from the plate boundary, resulting in some crustal thickening and minor erosion. In the north, continental crust has moved away from the collision zone along transforms to be placed over adjacent subducted oceanic lithosphere of the same plate, and the major process accommodating excess continental lithosphere is overthrusting of continental crust, accompanied by subduction of the lower part of the lithosphere. In the central South Island, accommodation of excess continental crust is by crustal thickening and erosion. Rock uplift at rates of about 11 mm/yr at the Alpine fault is balanced by erosion producing some 0.35×10^6 km^3 of sediment deposited mainly over the Challenger Plateau immediately west of the South Island. Some of the excess continental crust in this part of the plate boundary is accommodated as a root to the Southern Alps. On the basis of a number of observations it is argued that a 5-km-thick tabular body of high-grade schist near the middle of the Alpine fault is being extruded from the lower crust at a higher velocity than the plate convergence rate because (1) ductile lower crust outcrops in a highly condensed section, (2) fluid inclusion studies indicate temperatures as high as 360°C at depths of around 6 km, (3) stretching lineations in young mylonites show that motion normal to the Alpine fault is equal to, or faster than, the strike-slip component, and (4) a normal fault bounds the upper surface of the body, and the reverse Alpine fault bounds the lower surface. A similar process occurs in other convergent continental zones. While large earthquakes are known to have occurred on those parts of the Alpine fault north and south of the central segment of the plate boundary, it is unclear whether great earthquakes have been, or can be, generated on middle reaches of the fault, where the structure of the Alpine fault differs markedly and high temperatures are believed to exist close to the surface.

1. INTRODUCTION

Plate boundaries through continental lithosphere are usually broad, and the relative motion between plates is accommodated by diffuse deformation on a large number of structures; the plate boundaries south of the Eurasian plate and west of the North American plate are particularly clear examples. Relative motion between the Pacific and Australian plates across the Alpine fault through the South Island of New Zealand, however, is tightly constrained to the close vicinity of the fault, at least in the central parts, with a more diffuse deformation to the north and south. A study of the nature of the deformation to determine the actual modes by which relative plate motion in the South Island is taken up can be expected to throw light on processes of deformation in continental lithosphere in general through its marked contrast with the broader-scale deformation that occurs elsewhere.

Quantitative information published in the last 2 decades on the deformation that has occurred within the plate boundary zone through the South Island of New

Reviews of Geophysics, 36, 1 / *February 1998*
pages 1–26
8755-1209/98/97RG-03084*$15.00*
Paper number 97RG03084

TABLE 1. Finite Rotation Parameters, Southwest Pacific

Anomaly	Age, Ma	PAC-ANT			ANT-AUS			PAC-AUS = PAC-ANT + ANT-AUS		
		Latitude	Longitude	Angle, deg	Latitude	Longitude	Angle, deg	Latitude	Longitude	Angle, deg
1	0.78	64.25	−79.06	0.68	13.2	38.2	0.51	58.56	1.69	0.85
2a	2.58	67.03	−73.72	2.42	13.0	37.9	1.59	59.62	0.84	2.98
3a	5.89	67.91	−77.93	5.42	12.9	37.4	3.58	60.18	0.12	6.64
4a	8.86	69.68	−77.06	7.95	12.6	37.0	5.36	59.42	2.15	9.88
5r*	10.95				12.5	36.7	6.62			
5a	12.29	71.75	−73.77	10.92	13.0	35.7	7.40	58.53	3.17	13.85
5d	17.47	73.68	−69.85	15.17	14.1	33.6	10.34	57.60	2.70	19.75
6r*	20.13				14.5	32.8	11.98			
6c	24.06	74.72	−67.28	19.55	14.1	32.8	14.52	55.03	3.57	26.44
10	28.28	74.55	−67.38	22.95	13.8	32.7	17.24	54.10	2.17	31.08
13*	33.06				13.4	32.7	20.40			
13	33.54	74.38	−64.74	27.34	13.7	32.5	20.62	52.77	0.56	37.20

Finite rotation parameters for PAC-ANT motion [from *Cande et al.*, 1995]; anomaly numbers and their ages (based on *Cande and Kent* [1995]) are listed in the two leftmost columns. The rotations for anomalies used by *Cande et al.* [1995] are determined by linear interpolation based on the age of the anomaly. Finite relative rotations of Pacific and Australian plates in the final columns are calculated by composition [*Le Pichon et al.*, 1973] of PAC-ANT and ANT-AUS rotations.

*Data from *Royer and Sandwell* [1989]; ages have been adjusted to fit the *Cande and Kent* [1995] timescale.

Zealand is summarized from several disciplines. Detailed, well-constrained studies that incorporate many different fields, such as petrology, field geology, seismology, and geophysical modeling, are important in understanding the processes of deformation in continental lithosphere during collision.

There has been extraordinarily intense activity in the last 5 years with a sustained effort in the acquisition of field data. Overseas and New Zealand institutions have cooperated to conduct interrelated investigations. To date, more than 860 geodetic stations have been surveyed with high-precision Global Positioning System (GPS) (at least three 8-hour recording sessions on each), and half have been repeated after periods of a year or so at least once, some twice. About 72 Gb of three-component broadband seismic data have been collected. A further 80 GB have been collected from two multichannel reflection-refraction profiles across the waist of the South Island, involving 23 refraction and 40,000 air gun shots and a further 2000 km of offshore multichannel seismic profiles.

The purpose of this review is not to present these largely unpublished data but to provide a summary of what is currently known and understood about past deformation from already published material. Its aim is to provide an account of the present-day plate boundary and its geologically recent history so as to place the new work and their analyses in the context of the tectonic evolution of the plate boundary. The first part reviews recent work on the plate tectonics of the South Pacific to determine the scale of the problem: just how much shortening and strike-slip motion between the two plates on either side of New Zealand has there been, and how is it distributed in time? The bulk of the review is concerned with the dominant modes by which the oblique compression has been accommodated. There are many different structures active within a plate boundary, but only a few are important in accommodating the consumption of continental lithosphere, and attention is focused on those.

Several recent papers successfully address general issues of South Island tectonics, most notably those of *Norris et al.* [1990] for the south and central South Island, *Lamb and Bibby* [1989] for the north, and *Anderson et al.* [1993] for major historical earthquakes throughout the South Island. Much information in these papers is not duplicated here and they provide invaluable information.

2. PLATE TECTONICS OF THE SOUTH PACIFIC

New information on the plate tectonics of the South Pacific available in recent years gives greatly improved resolution of relative plate motion over that of even 5 years ago. Radar altimetry data from Seasat, Geosat, and ERS-1 [*Haxby*, 1987; *Sandwell and Smith*, 1995] give improved estimates of the direction of motion along the Pacific-Antarctic (PAC-ANT) and Australian-Antarctic (AUS-ANT) plate boundaries, and a new chronology of magnetic anomalies [*Cande and Kent*, 1992, 1995] gives improved age control. *Cande et al.* [1995] give magnetometer and multibeam bathymetry from the Pitman fracture zone on the Pacific-Antarctic (PAC-ANT) plate boundary and present refined estimates of the finite rotation parameters for the PAC-ANT boundary. These, although similar to earlier estimates [*Stock and Molnar*, 1987] show small but significant changes in the direction and rate of spreading on the PAC-ANT boundary since the Cretaceous. *Royer and Sandwell* [1989] have redefined the plate tectonic history of the ANT-AUS pair of plates also, and both boundaries together permit the estimation of motion on the PAC-AUS boundary to much greater resolution than before. Finally, plate motion

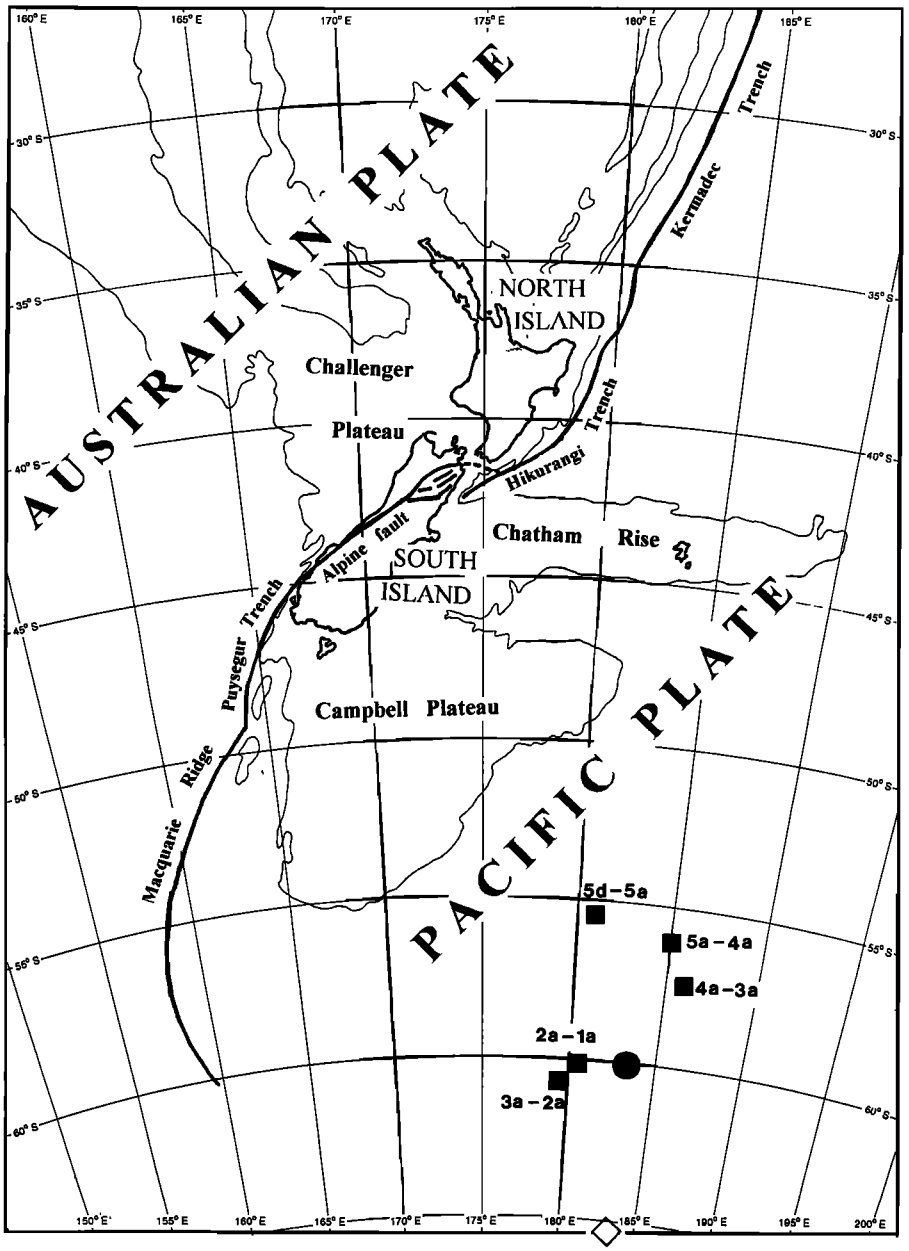

Figure 1. Plate boundary of the Pacific and Australian plates. The Pacific plate has rotated counterclockwise relative to the Australian plate about poles (solid squares), the positions of which have changed progressively with time. The poles for motion during the period of magnetic anomalies 5d (17.5 Ma) to 3a (5.89 Ma) indicate fault-parallel motion on the Alpine fault, whereas since anomaly 3a the poles are located well to the southwest of their earlier position and indicate an additional compressional component of motion across the Alpine fault. The NUVEL 1 pole, obtained from seafloor spreading information, is the solid circle, and the geodetically determined GPS pole is the open diamond.

has now been measured directly using high-precision global geodetic techniques [*Larson and Freymueller*, 1995].

2.1. History of Plate Kinematics in the South Pacific

Both Pacific and Australian plates are moving away from Antarctica by spreading on the mid-oceanic rise south of Australia and New Zealand. They move in slightly different directions and speeds, so there is a resultant motion of one relative to the other involving convergence or strike-slip motion along their common (PAC-AUS) boundary. New estimates of the relative motion of the Pacific, Australian, and Antarctic plates are given in Table 1. To produce a uniform set of anomalies and rotation parameters, it is necessary to interpolate values for AUS-ANT plate boundary. The AUS-ANT finite rotation poles have changed little in position over the last 10 Myr and the present-day rate of plate motion of 0.65°/Myr is close to the average rate given by the anomaly 5 finite rotation, 0.60°/Myr. Because the ANT-AUS rotation vector changes little, interpolation introduces very little error.

2.1.1. PAC-AUS motion. Relative motion of the Pacific and Australian plates is computed from the plate circuit PAC-ANT-AUS. This procedure assumes that there is no motion between East and West Antarctica, such as that suggested by *Sutherland* [1995] for the middle Cenozoic. There is certainly no evidence of deformation between the two today in the complete lack of seismicity there. The poles of the finite rotations for PAC-AUS motion are listed in Table 1. Stage rotations give an estimate of the direction and rates of motion over a specified time interval relative to one of the plates, in this case the Australian plate. The stage poles are shown in Figure 1 as solid squares. From anomaly 5d

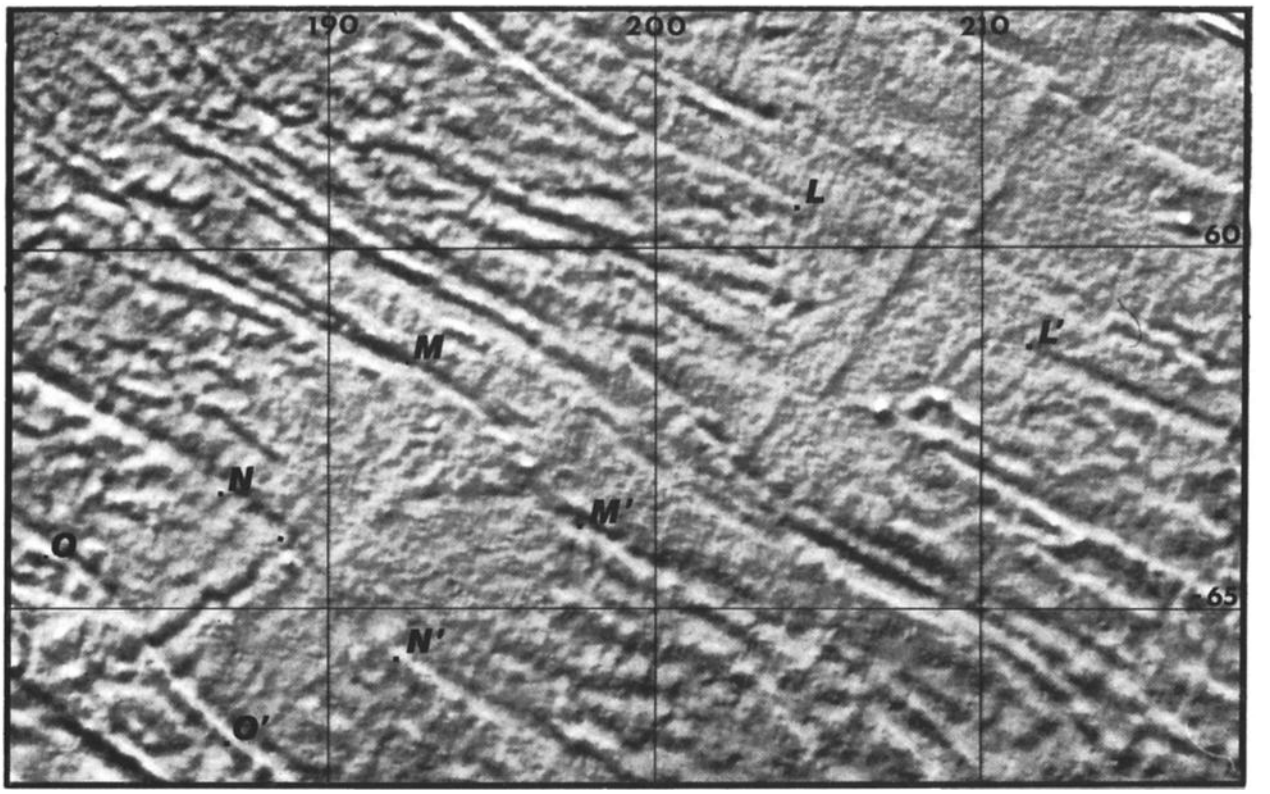

Figure 2. Gravity anomaly map of the Pacific-Antarctic plate boundary south of New Zealand between 58° and 67°S and 180° and 220°E, from *Sandwell and Smith* [1995]. Letters L, M, N and O are points on the Pacific plate where a change in direction of plate spreading can be seen in the gravity anomaly trends. The primed letters are the equivalent positions on the Antarctic plate. A rotation about the *Cande et al.* [1995] pole for anomaly 3a gives the best fit in rotating the two sets of points to overlap, but an angle 8.5% greater than the finite angle of rotation for 3a is needed.

time (17.5 Ma) to anomaly 3a time (5.89 Ma) the stage poles moved directly away from New Zealand along a perpendicular to the Alpine fault, and the rate of rotation remained steady at about 1.1°/Myr. Hence the Alpine fault was a small circle to the pole throughout this period, and the rate of dextral slip across the plate boundary zone in the central South Island has increased with time (from 35 to 38 mm/yr). The major change in position of the 4a and 3a stage poles indicates a change in the direction of motion along the New Zealand plate boundary. The precise age when the position of the pole first started to change can be best estimated from the satellite gravity map (Figure 2) of the PAC-ANT boundary. This gravity map shows the trends of fracture zones produced at transform faults of the spreading center. An inflection in the trend occurs across the present spreading center. The position of four points on particularly clear trends near the limits of the inflection are shown as letters L, M, N, and O on the Pacific plate and as the same letters with primes on the Antarctic plate. The finite rotation pole that best fits the points on the Pacific plate to the equivalent points on the Antarctic plate is that for anomaly 3a but with a rotation angle of 5.88°, which is 8.5% larger than the rotation angle for 3a. The estimated time for the initiation of change in direction of plate motion is therefore 8.5% older than anomaly 3a, or 6.4 Ma. *Cande et al.* [1995] estimate the age at which the change occurred as the young end of anomaly 3a, i.e., 5.89 Ma, from observed changes in abyssal hill azimuths. Before about 6 Ma, motion across the Alpine fault was almost purely strike-slip, and since then there has been a substantial compression as well.

2.1.2. Total amount of shortening across the South Island. The motion of three points 200 km apart on the Alpine fault, corresponding to present-day positions at 44.5°S and 168°E near Milford Sound, 43.5°S and 170°E in the middle, and 42.5°S and 172°E near the northern end of the straight part of the Alpine fault, is shown in Figure 3 using the data of Table 1. Convergence across the Alpine fault commenced at 6.4 Ma, and the total convergence during this period has been around 90 km in the center, with 70 km at the southern end and about 110 km at the northern end of the Alpine fault. Before 6.4 Ma the motion of the Pacific plate was nearly parallel to the present trend of the Alpine fault, with a small component of convergence of only a few millimeters per year. Though the rate is small it still amounts to 25 km of shortening in the 12 Myr prior to the onset of rapid shortening.

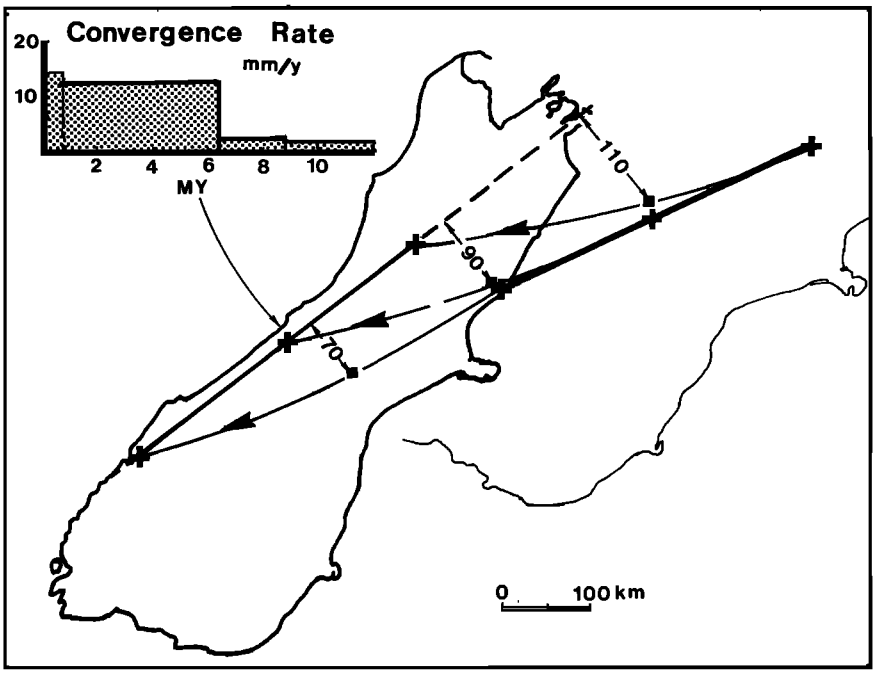

Figure 3. The Pacific plate's motion relative to the Australian plate since anomaly 5c time (12.4 Ma). The diagram shows the present-day location of three points on the Alpine fault and where they would have been at 6.4 Ma (solid squares) and 12.4 Ma (crosses). From 12.4 to 6.4 Ma, motion was almost purely strike-slip, but since then the rate of shortening normal to the Alpine fault has averaged 13 mm/yr as shown in the graph. There has been a total of 90 km compression since 6.4 Ma in central Alpine fault, with 110 km in the north and 70 km in the south.

2.2. Present-Day Plate Motion

Present-day plate motion of the PAC-AUS plate boundary has been measured directly [*Larson and Freymueller*, 1995; *Larson et al.*, 1997] and is independently inferred from seafloor spreading data [*Chase*, 1978; *De Mets et al.*, 1990]. Although at most other boundaries the two methods give the same values within their respective errors, they differ significantly for the Pacific plate and the PAC-AUS boundary in particular. The direct measurement of plate motion is based on the Global Positioning System. The position of the GPS pole is at latitude 65.7°S and longitude 182.9°E, and the rate of rotation is 1.04°/Myr [*Larson et al.*, 1997] using the permanent network stations of the International GPS Service for geodynamics. The error in position is about 1.5°, and the error in rate is 0.02°/Myr.

Seafloor spreading data have resulted in a number of global kinematic models of plate motions, the most recent one being NUVEL 1 [*DeMets et al.*, 1990]. This model, modified in 1993 as NUVEL 1A to incorporate new information on dating [*DeMets et al.*, 1994], is the standard reference for plate kinematics. The NUVEL 1A Euler vector for Pacific-Australian plate motion is 60.1°S, 181.7°E (Figure 1), and the rate of rotation is 1.07°/Myr. The GPS pole differs in position by some 5° from the NUVEL 1A pole. Because the pole is close to New Zealand, a small change in its position results in a large change in the computed relative motion of the plates across the New Zealand plate boundary.

The consequences of the difference in pole position are most marked in considering the contemporary rate

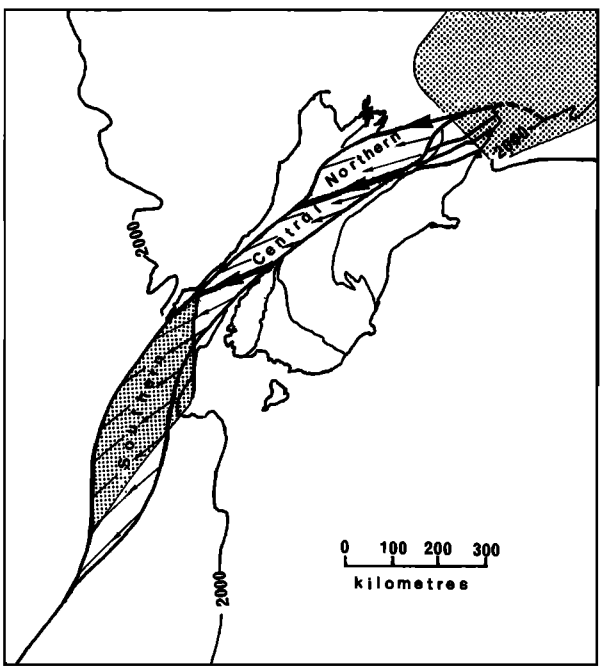

Figure 4. Excess lithosphere at 6.4 Ma and the amount lost since that time. The amount and direction of motion of the Pacific relative to the Australian plate is shown by arrowed lines representing small circles about the 3a finite pole. Displacements are 190 km south of the plate boundary and 230 km north of the boundary. Subducted oceanic lithosphere is shown by the coarse dot screen. The 2000-m depth contour indicates the boundary between oceanic and continental crust. Three segments of the plate boundary are shown and identify the three areas in which the excess lithosphere is accommodated by different processes.

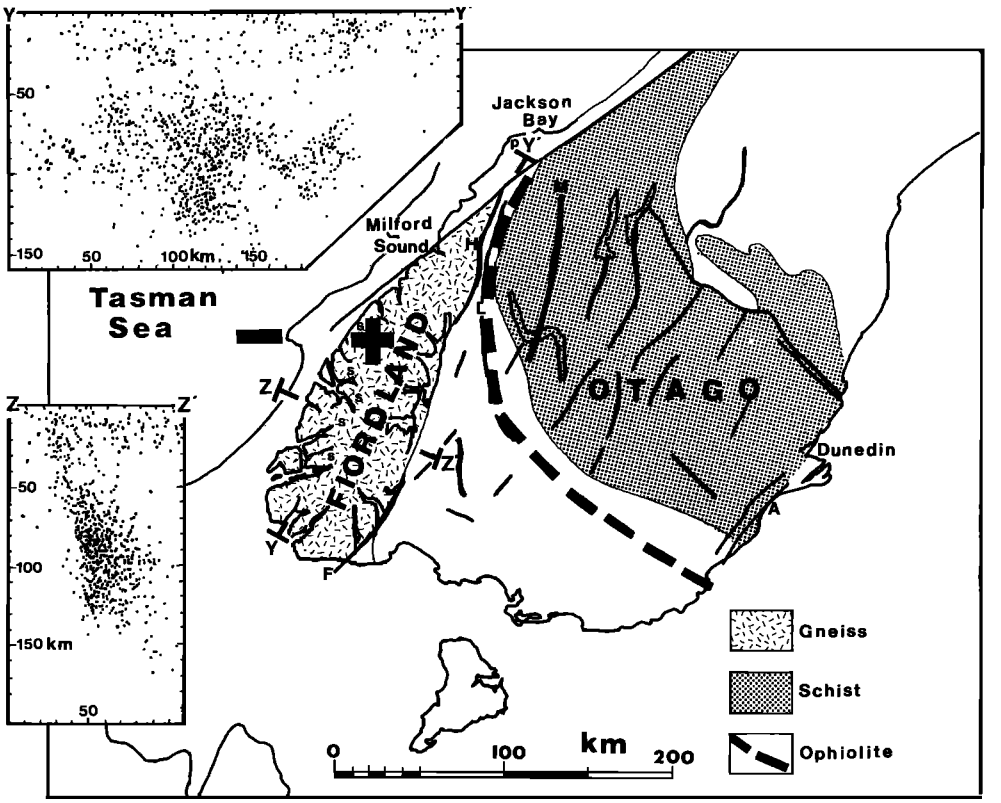

Figure 5. Southern South Island structure. The Fiordland block is not part of the Pacific plate, and the plate boundary extends to the east coast with widespread, low-intensity deformation on NE-SW and NW-SE trending reverse faults. The ophiolite belt is strongly curved. The bold plus and minus signs show the locations of 150-mgal gravity anomaly high and low related to the Fiordland subduction zone. Profiles of earthquake locations in the subducted plate under Fiordland from *Anderson et al.* [1993] are inset. The offset in location of source rocks (shown by letter s) from a late Pliocene conglomerate (letter p) indicates a slip rate on the Alpine fault of about 35 mm/yr [from *Sutherland*, 1994].

of shortening across the Southern Alps and Alpine fault. NUVEL 1A predicts motion at the middle of the Alpine fault, at −43.5°S and 170°E, with a direction inclined at 16° to the Alpine fault and a shortening rate of 10 mm/yr. The GPS pole indicates a direction inclined at 22° and a shortening rate of 16 mm/yr. The long-term average motion determined from anomaly 3a finite rotation is 18° in direction and 13 mm/yr in rate of shortening. It is the long-term average that is used in subsequent calculations.

3. MODES OF OBLIQUE COMPRESSION IN CONTINENTAL LITHOSPHERE

While the relative position of the Pacific and Australian plates can be reconstructed with considerable confidence at any time during the late Cenozoic, the reconstruction of the deformed zone between the plates is much more difficult. It is a straightforward procedure, however, to calculate the total amount of displacement over any period of time, and the problem of reconstruction within a plate boundary zone reduces to identifying those modes of deformation responsible for accommodating the displacement. The reconstruction of Figure 4 shows the change in position between the present and 6.4 Ma at the beginning of the change in direction of Pacific plate motion relative to the Australian plate. The plate boundary through New Zealand is taken to be the Alpine fault from the Hikurangi Trough in the north to Milford Sound (Figure 5) in the south and beyond to the Puysegur Trench and the Macquarie Arc. The displacement between then and now is shown by arrowed lines; the amount of displacement is 190 km in the south and 230 km in the north. This lost lithosphere must have been largely continental because of continuity in structures, such as a Permian ophiolite belt (Figure 5), across the plate boundary. Like the present-day continental crust of the Challenger and Campbell Plateaus, it would consist of crust about 25 km thick. How this lithosphere came to be consumed during oblique compression of the plate boundary zone is the problem addressed in the rest of the paper.

The modes by which excess lithosphere within the plate boundary zone is accommodated during compression differ in different segments of the plate boundary, named here the southern, central, and northern segments. The central and northern segments of the plate

boundary zone involve oblique collision of continental lithosphere. The southern segment involves, in part, subduction of oceanic lithosphere (shown shaded in Figure 4), which accommodates much, but by no means all, of the excess lithosphere in that segment.

3.1. Southern Segment

The southern segment extends from the Macquarie Arc northward along the Puysegur Trench and Alpine fault to the northern tip of the Fiordland block. The area of lithosphere lost in the Pliocene-Quaternary compression is 54,000 km^2. Most is accommodated by subduction of oceanic lithosphere of the Australian plate. The area of the subducted oceanic lithosphere is 45,000 km^2 (Figure 4), of which only a small part, if any, would have been subducted before 6.4 Ma. The remaining 9000 km^2 is accommodated by distributed crustal thickening east of Fiordland, mostly in western Otago (Figure 5).

3.1.1. Fiordland. Fiordland is a broad plateau of crystalline rocks about 1000 m in elevation, interrupted by deep glacially carved fiords and valleys, that was covered by a local ice cap and distributary glaciers during the Pleistocene. It abuts, across the Alpine fault to the northwest, oceanic lithosphere of the Tasman Sea. One of the largest paired gravity anomalies in the world occurs here, with free air anomaly of −150 mgal over the deep sea and Bouguer anomaly of +150 mgal over central Fiordland. Fiordland is underlain by subducted oceanic lithosphere of the Australian plate, and intense seismic activity in the subducted lithosphere shows that the subduction is still active (Figure 5).

3.1.2. Deformation east of Fiordland. Fiordland is not part of the Pacific plate. Seismic activity occurs along its eastern boundary; *Anderson et al.* [1993] list one (6.2 M_s) strike-slip event, and seismicity, although weak, is present as far east as the Akatore fault on the coast south of Dunedin. In central and eastern Otago, geodetic strain rates [*Walcott*, 1978, 1984; *Reilly*, 1990] are small, about or less than 0.1 μstrain/yr, equivalent together with the geodetic strain immediately east of Fiordland measured by *Pearson* [1992] to a displacement rate of 10 mm/yr across the full width of the deforming zone and sufficient to account for all present-day shortening.

NW-SE shortening is obvious geologically throughout the southern South Island to a distance of 200 km from the Alpine fault [*Yeats*, 1987]. Distributed deformation in eastern Otago accounts for only part of the total 70 km of shortening required between Fiordland and the Pacific plate, perhaps only about 10 km in all [*Norris et al.*, 1978], and most of the deformation accommodating the shortening must occur in mountainous terrain adjacent to the east boundary of the Fiordland block. There, immediately east of Fiordland, extensive late Cenozoic deformation involves faults of north-south (e.g., Hollyford and Livingstone faults) and NE-SW (e.g., Moonlight and Fiordland Boundary faults) trend. Strike-slip movement is described for the NE-SW faults with some

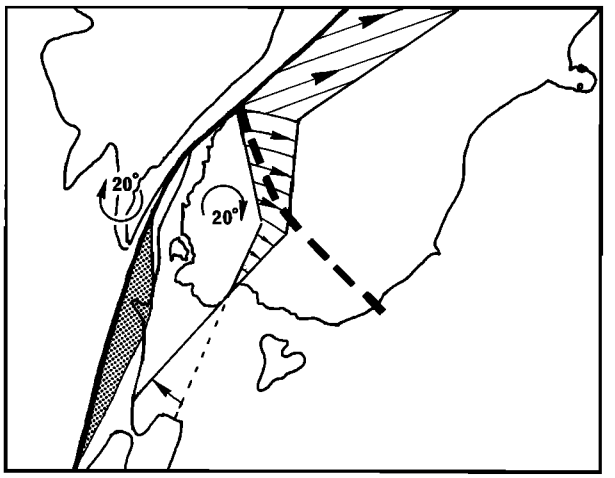

Figure 6. Reconstruction of the southern segment of the plate boundary zone at 6.4 Ma. Fiordland is rotated through 20° to keep it adjacent to the edge of the Australian plate, thus requiring most of the 70 km of shortening to be accommodated east of Fiordland. Southern Westland is also rotated through 20° to close a gap that would otherwise appear. The subducted plate at 6.4 Ma is shown by coarse stipple. The ophiolite belt (Figure 5) would have been almost straight in the Miocene.

20 km of dextral displacement [*Norris and Turnbull*, 1993]. Late Cenozoic shortening has resulted in faulting and folding of Oligocene and Miocene and older strata and, judging by the mountainous nature of the country, crustal thickening. *Norris and Turnbull* [1993] give a palinspastic reconstruction involving some 30 km of shortening on north-south trending reverse faults. A horizontal detachment near the base of the crust, as modeled by *Koons and Henderson* [1995] for the folding of central Otago, could be associated with shortening in the crust but of course does not account for the shortening in the lithosphere as a whole: if a detachment exists, then the part of the lithosphere below it must either be subducted or be accommodated by some other mechanism.

3.1.3. Reconstruction at 6.4 Ma. Judging by the degree of deformation of the rocks east of Fiordland, the total amount of NW-SE shortening decreases southward, indicating probable rotation of the Fiordland block relative to the Pacific plate. This is the interpretation made in reconstructing southern New Zealand in Figure 6. The Fiordland block lay immediately adjacent to the Alpine fault and the Australian plate during the late Cenozoic, so that the deformation required to accommodate the compression across the plate boundary zone occurred on its eastern side. A distinctive belt of Permian ophiolitic rocks and associated magnetic anomalies identified in Figures 5 and 6 by a heavy dashed line illustrates how the distributed deformation east of Fiordland resulted in, or accentuated, the curved arcuate structure of present-day southern South Island. It is also proposed in Figure 6 that the southern end of the west coast, south of Jackson Bay, has rotated about 20°

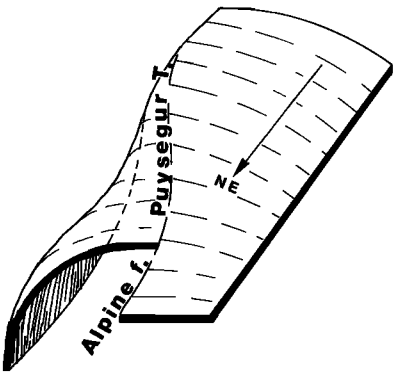

Figure 7. The Fiordland subduction zone "ploughshare" [after *Christoffel and van der Linden*, 1972].

counterclockwise, a process continuing today as can be seen in earthquake slip vectors (Figure 12).

Displacement of Fiordland in the direction of the plate boundary (NE-SW) could also have occurred. For example, the Fiordland block may have been extruded southwestward from the boundary zone during compression and so have moved faster relative to the Australian plate than the Pacific plate itself. However, the sinistral shear that would be necessary between Fiordland and the Pacific plate has not been identified, nor is it evident in earthquake source mechanism and geodetic investigations. Dextral shear on the NE-SW Moonlight fault system has been commented upon by *Norris et al.* [1978], in which case Fiordland would have moved slower relative to the Australian plate than the Pacific plate, but this is considered by them to be subordinate to NW-SE shortening. *Norris et al.* [1990] consider that deformation east of Fiordland is consistent with a northward relative movement of Fiordland, but again the amount is unclear.

3.1.4. The Fiordland subduction zone. Between the Macquarie Arc, where the plate boundary is subparallel to the direction of relative plate motion, and the west coast of the South Island, the plate boundary bends northward around the Fiordland block in the Puysegur Trench. Intermediate-depth earthquakes under Fiordland show that a part of the Australian plate has been subducted at the Puysegur Trench. The deepest earthquakes lie 150 km under Fiordland (Figure 5). *Christoffel and van der Linden* [1972], who first investigated the Fiordland subduction, described the subducted plate as shaped like a ploughshare, and this remains an accurate description (Figure 7). The subducted plate is a flake of oceanic lithosphere, a corner of the Australian plate, that has been thrust longitudinally under the southwest corner of the South Island. The paired gravity anomalies result from the northward movement of the ploughshare tilting the Fiordland block and lifting its edge by about 3 km, with a compensating downward flexure of the Australian plate. Most, if not all, of the subduction has occurred in the last 6.4 Myr. The time when subduction was initiated is not obvious because the motion of the Fiordland block is poorly constrained. The subducted plate extends a distance of 250 km from the Puysegur Trench in the direction of relative plate motion, requiring subduction to have commenced at some time between anomalies 3a and 5a. From the length of subducted plate and the speed of relative plate motion, subduction is estimated to have commenced around 10 Ma; i.e., 10 Myr ago the northern edge of the subducted plate would have cleared the southern edge of the Fiordland block [*Davey and Smith*, 1983]. This presumes that the Fiordland block has moved with the Pacific plate, which may not be true; if it lay only slightly farther north relative to the Pacific plate and had rotated around 20° counterclockwise, then subduction may have commenced within the last 6.4 Myr. On the other hand, if Fiordland lay in much the same position relative to the Pacific plate, or even farther south, then subduction needs to have started before 6.4 Ma. The subducted oceanic lithosphere is Oligocene in age, produced at the Australian-Pacific plate boundary around 40 Ma [*Sutherland*, 1995, Figure 3], so negative buoyancy would be small.

3.1.5. Rate of slip on the Alpine fault. *Sutherland* [1994] describes Pliocene sediments on the west coast of the South Island (shown by "p" in Figure 5), on the Australian plate, containing clasts derived from source rocks in central and southern parts of the Fiordland block (shown by "s" in Figure 5) that today lie on the opposite side of the Alpine fault, 100 km to the southwest. A minimum rate of slip of the Fiordland block of 35 ± 5 mm/yr is estimated. This is similar to the relative motion of the Pacific and Australian plates, suggesting that the Fiordland block has not moved substantially in the direction of the plate boundary relative to the Pacific plate. Given the nature of the data with uncertainties in both source position and timing, the quoted 5-mm/yr constraints on the speed, particularly with regard to the upper limit, are too small.

3.2. Northern Segment

Hope fault, the most southerly of the major strike-slip faults of northeastern South Island, is the southern boundary of the northern segment. The Wairau fault and its probable continuation down Cook Strait between North and South Island [*Walcott*, 1978; *Carter et al.*, 1988], is the northern boundary (Figure 8). The Hope fault meets the Alpine fault near Arthur's Pass 300 km from the tip of the Fiordland block and 250 km from Cook Strait. Extensive late Cenozoic deformation extended up to 200 km on both sides of the Alpine fault, and the fault itself is bent through about 20 km as a consequence of this deformation. The style of deformation differs across the Alpine fault; in the west, Miocene to recent reverse faulting has resulted in crustal thickening and uplift of a Late Cretaceous erosional surface with moderate erosion; on the east, uplift and erosion are secondary to northeastward directed overthrusting

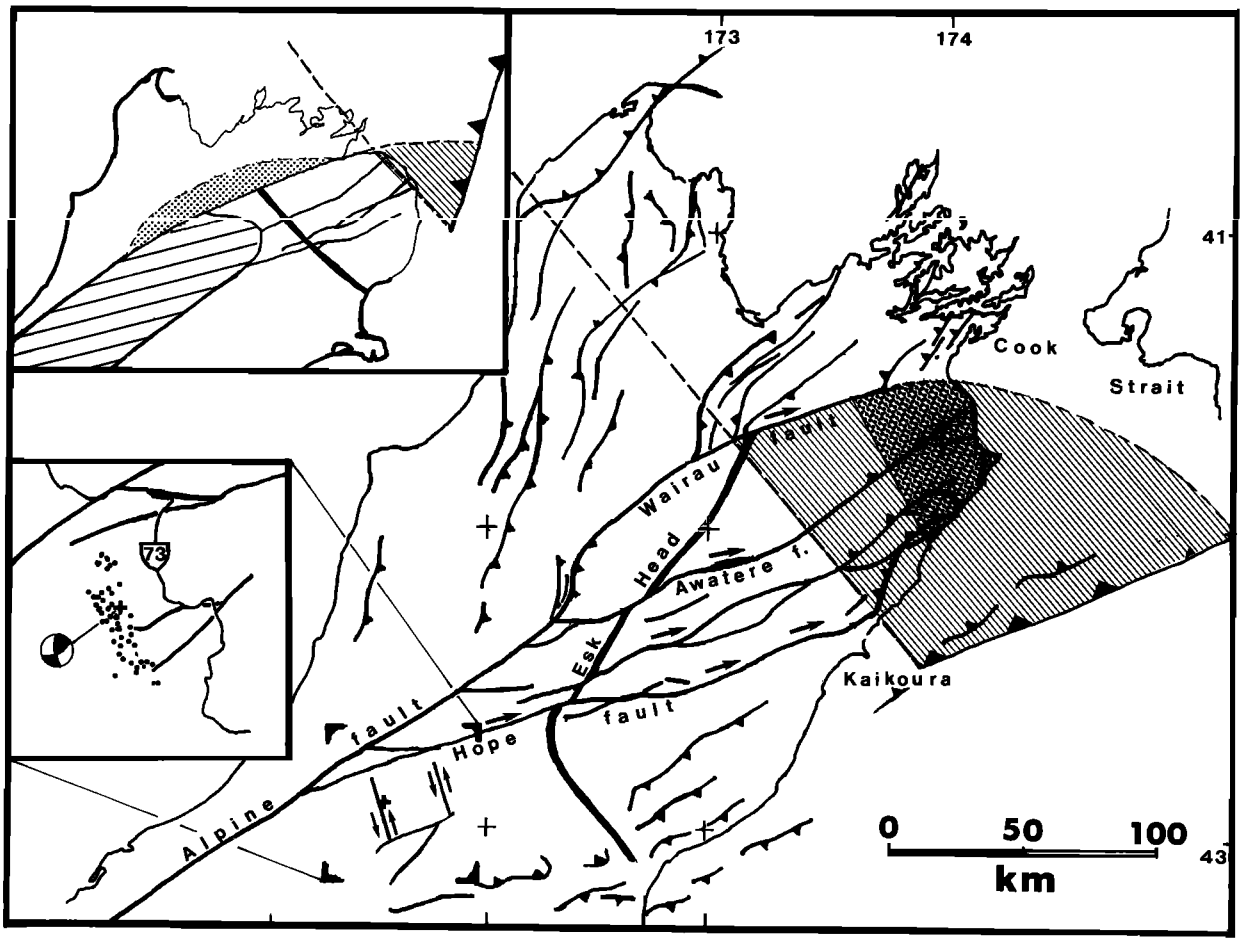

Figure 8. Northern segment of the plate boundary zone extends from the intersection of the Hope and Alpine faults to Cook Strait. Pliocene-Quaternary deformation is widespread across the full 250-km width of the northern part of the South Island. The dashed line is the southern limit of the subducted Pacific oceanic lithosphere. The most remarkable feature of this region is the large amount of Pacific continental crust that now lies on subducted oceanic lithosphere of the same plate (hatched). Part of the overthrust crust, at least as large as the part shown in coarse stipple, has rotated clockwise about 30° since 6.4 Ma, as is shown by paleomagnetic declinations [*Little and Roberts*, 1997]. Between the Alpine fault and the southern edge of the subducted plate, faults parallel to the direction of plate motion are continental transforms transporting lithosphere from the collision toward the overthrust zone. The top inset shows the northern segment reconstructed at 6.4 Ma by rotating and aligning the Esk Head marker (solid line) to be parallel to the southwestern edge of the subducted plate. The area lost by uplift and erosion is heavily hatched. The fine-hatched area is the obducted crust of the time. The stippling shows the area lost by compression within northwest South Island. The bottom inset shows well-determined aftershocks of the 1993 Arthur's Pass earthquake from *Robinson et al.* [1995] revealing left-lateral cross faults. The location of the main shock is shown together with the location of highway 73.

of continental crust in accommodating crustal consumption. The total area of continental rocks lost in the Pliocene-Quaternary is about 25,000 (= 250 × 100) km^2, and that lost since the mid-Miocene is about 30,000 (= 250 × 120) km^2.

During early Cenozoic time the east coast of the North Island and the northeastern South Island occupied a passive continental margin with deposition of bathyal clays and muds, deepwater limestone, and minor sands. In early Miocene time the sedimentation completely changed, with thick, coarse clastics including sedimentary melange, olistostrome, and thick turbidites accompanied by intense deformation and landward emplacement of allochthonous sheets of the passive margin sequence [*Rait et al.*, 1991]. The Tonga-Kermadec subduction zone is believed to have propagated southward to New Zealand at this time and has been active ever since. The occurrence near Kaikoura of the Great Marlborough conglomerate, a thick formation of sedimentary melange that at least in part, is 18 Myr old and contains clasts of the entire foregoing passive margin sequence, indicates vigorous synsedimentary deformation. Presumably, subduction occurred this far south early in the Miocene.

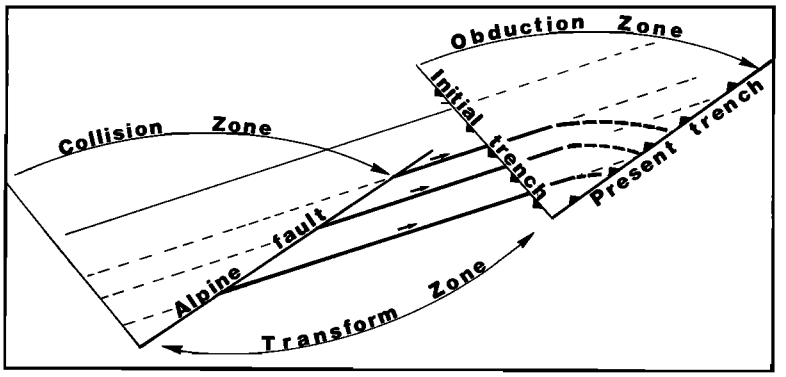

Figure 9. Cartoon illustrating how lithosphere within the collision zone adjacent to the Alpine fault is carried by transform faults northeastward to thrust over onto the subducted Pacific plate in the overthrust zone.

3.2.1. Emplacement of continental crust onto the southern Hikurangi margin. The most remarkable feature of the northern segment is the large area of continental crust, once part of the Pacific plate, that now lies above subducted oceanic lithosphere of the same plate. The Benioff zone of the Tonga-Kermadec-Hikurangi subduction deepens northwestward from the Hikurangi Trough to about 250 km and extends northeastward toward the Kermadec and Tonga Arcs. It ends at a line trending northwest through Kaikoura (Figure 8). The southernmost edge of the subducted plate is identified by an abrupt step in the deepest earthquakes [*Anderson et al.*, 1993] from 250 km to less than 100 km deep and is aligned with the 2000-m bathymetric contour on the boundary of the continental lithosphere of Chatham Rise and the thinner, oceanic lithosphere of the Pacific Ocean. The edge marks the early Cenozoic passive margin that has become caught up in the Pacific-Australian plate boundary. The area of continental crust of the Pacific plate that has been obducted onto subducted oceanic Pacific lithosphere is shown hatched in Figure 8. It covers an area of 15,000 km^2 shaped as a quadrant of a circle with radius of 140 km. According to *Lamb and Bibby* [1989], overthrusting of Pacific plate continental crust commenced at the Hikurangi margin in earliest Miocene time by thrusting parallel to the NW trending margin. The rate of overthrusting increased in the Pliocene–Quaternary.

3.2.1.1. Reconstruction at 6.4 Ma: A reconstruction of the northern segment at 6.4 Ma is shown in the top inset of Figure 8. The coarse-hatched area is the excess crust accommodated by processes of crustal thickening and erosion. The fine-hatched area is the amount of crust estimated to have been overthrust up to that time. The reconstruction is made by sliding crust back along the Marlborough strike-slip faults until the Esk Head boundary, a major structural and lithological boundary that currently trends NNE, is aligned parallel to the southwestern edge of the subducted oceanic plate. Whether this alignment had occurred by 6.4 Ma is not known. If it had, about half of the continental crust lost in the last 6.4 Ma is accommodated by overthrusting. The mechanism by which the segments of the Esk Head boundary between the major strike-slip faults rotated from their initial NW-SE trend to the current NNE-SSW trend is discussed below.

3.2.1.2. The Marlborough faults: The Marlborough fault system comprises three different modes of deformation, illustrated in the cartoon of Figure 9.

1. In the overthrusting, or obduction, zone northeast of the edge of the subducted plate, oblique slip across the major fault results in crustal thickening, uplift of the major ranges, and erosion. Near the coast of Cook Strait and the Pacific Ocean the motion on the fault dies out against a rotating, obducted, block of continental crust lying on the subducted plate.
2. The central section, the transform zone, comprises conservative faults that move the excess lithosphere of the Alpine fault collision zone toward the overthrusting zone to the northeast.
3. The collision zone is where the western sections of the faults lie within the strongly deformed Southern Alps. They splay outward and disappear as identifiable faults in the strongly deformed rocks adjacent to the Alpine fault. Offsets of some lithologic boundaries are shown on maps (Figure 13), but these are small compared with the several tens of kilometers needed to produce the large amount of obducted crust. A different process is needed in order to produce the movement of large amounts of lithosphere away from the collision zone.

3.2.1.3. Collision zone: Recent earthquakes reveal details of the process by which lateral expulsion of the crust from the northern segment of the continental collision zone is achieved. The 1994 Arthur's Pass earthquake occurred within a network of GPS stations established a few months earlier, and the mechanism was tightly constrained by the observed displacements. The earthquake occurred on a NNW trending cross (antithetic) fault, as was shown by the distribution of aftershocks (Figure 8b), and was sinistral in offset [*Robinson et al.*, 1995; *Árnadóttir et al.*, 1995].

In 1996 a similar earthquake, the Cass earthquake, occurred 20 km farther east and is presumed to lie on the eastern edge of the tabular block of which the Arthur's Pass earthquake was on the western edge. The cross faults end against major dextral faults that trend parallel to the plate motion vector, in the south against

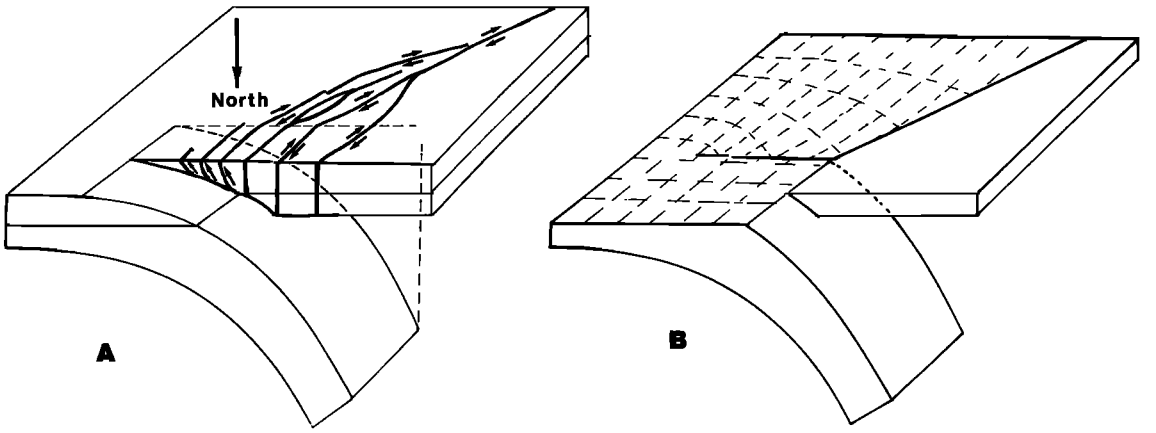

Figure 10. (a) Structural model of the northeastern South Island after *Bibby* [1981] showing how the motion on faults is believed to be partitioned into strike-slip behind, and reverse faulting at the front of the subduction zone. The faults in plan view can be seen in the map of Figure 8. (b) The upper crust is removed and only the lower lithosphere is shown. Lower continental lithosphere is subducted under the oceanic lithosphere.

the incipient Porter's Pass fault zone and in the north against the westward extension of the Hope fault. The Hope fault last moved in a large earthquake in 1888 [*Cowan*, 1990]. *Cowan* [1990] identifies a similar structural association of through going dextral faults with blocks bounded by cross faults throughout the zone of transform faulting. This process of active cross faults and rotation of blocks does not seem to be active today north of the Awatere fault, and we may suppose that this activity has migrated southward with time as progressively more lithosphere is caught up in the plate boundary deformation. Thus the rotation between the Wairau and Awatere faults is presumed to be largely of Miocene age, and the rotation farther south is younger still, with the major activity today being south of the Hope fault.

3.2.1.4. Transform zone: Continental crust caught up in the convergence across the Alpine and Wairau faults has moved laterally along the Marlborough fault system toward the subducted edge of the Hikurangi subduction zone. In the last 20 years, new fault slip rate data have become available, particularly for the Marlborough faults. Fault slip rates are obtained by measuring a dated offset across the fault, and while the distance of offset can be measured with almost arbitrary precision, determination of age is exceedingly difficult. In the late 1970s the estimates of slip rate on the whole of the fault system amounted to less than one third of the plate motion. Since the geodetic strain rate equaled the plate motion rate, this led to the suggestion that two thirds of plate motion was accomplished by aseismic processes [*Walcott*, 1978]. *Holt and Haines* [1995] provide a summary of fault slip rates on the Marlborough fault system. Using kinematic modeling techniques [*Haines*, 1982], they show that when combined with rock uplift information, fault slip rates are sufficient to give a velocity of the Pacific relative to the Australian plate indistinguishable in direction and rate from the NUVEL 1A [*De Mets et al.*, 1994] kinematic model for plate motion. Evidently, those segments of the faults parallel to the present plate motion that lie SW of the overthrust crust take up the whole of the plate motion and are truly conservative faults.

3.2.1.5. Overthrust zone: The direction of transport of the continental lithosphere from the zone of collision at the Alpine fault toward the subduction zone is ENE, orthogonal to the southern edge of the subducted Pacific plate (Figure 8). Continental crust has been thrust onto the subducted plate for up to 140 km in the Wairau and Awatere region, and the fragment lying on the subducted surface (stippled area in Figure 8) has been rotated clockwise into its present position [*Lamb and Bibby*, 1989]. *Bibby* [1981] noted that geodetic strain axes systematically swung across the northern part of the South Island, resulting from a change in faulting style with northeast trending reverse faults in the east and subparallel strike-slip faults in the west (Figure 10a). This change indicated strain partitioning, with motion parallel to the plate boundary taken up on one set of faults and perpendicular motion taken up on another set. *Van Dissen and Yeats* [1991] showed, through structural mapping, that strike-slip motion on the Hope fault terminated in shortening across the Jordan thrust. *Lamb and Bibby* [1989] argued that the uplift of the Seaward and Inland Kaikoura ranges and others as well were the result of oblique slip on the northeastern ends of the major Marlborough faults. They showed that a swing in the trend of the Marlborough faults from parallel to the plate motion vector in the west through about 30° to a trend NW-SE in the east coincided with the southwest edge of the subducted Pacific plate. Strike-slip motion on the western portions of the fault was accommodated on the eastern faults in part by shortening and crustal thickening and in part by rotation of the oblique slip faults and crust.

3.2.1.6. Rotation of obducted crust: Most of the convergence across the southern edge of the Hikurangi

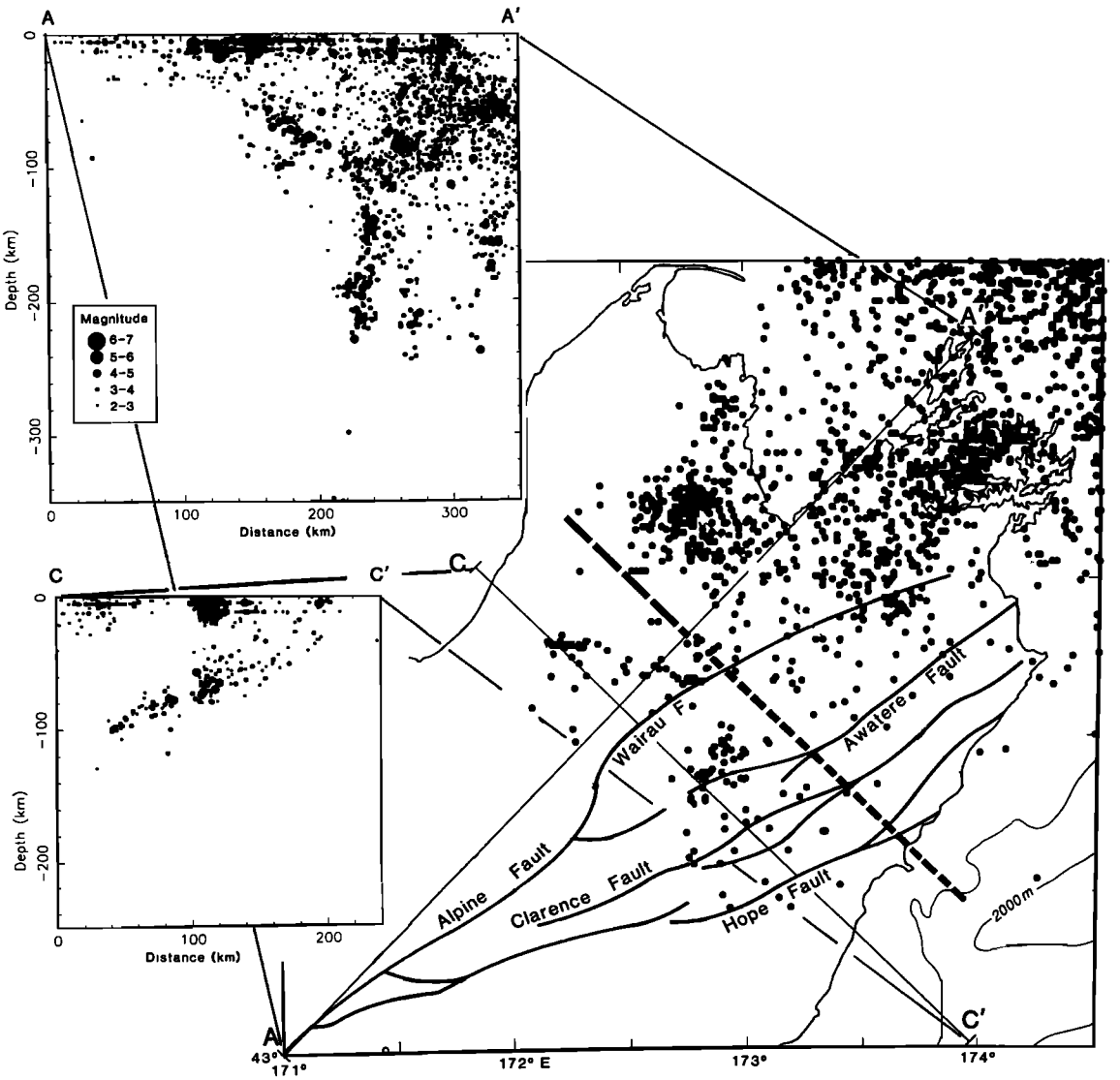

Figure 11. Seismicity under the northern South Island [from *Anderson et al.*, 1993]. The Tonga-Kermadec-Hikurangi subduction zone ends at the heavy dashed line and the abrupt shallowing of the deepest earthquakes from 250 to 100 km in depth shown in profile A-A'. Southwest of the dashed line a small Benioff zone dips to the north and can be seen in profile A-A' dipping northeastward and in profile C-C' dipping northwestward.

subduction has occurred in the last 4 Myr [*Lamb and Bibby*, 1989]. Rotation of the leading edge is seen in paleomagnetic studies and anomalous paleomagnetic declinations [*Walcott et al.*, 1981; *Roberts*, 1992, 1995; *Vickery and Lamb*, 1995]. Late Cenozoic sedimentary rocks in northeasternmost Marlborough have paleomagnetic declinations indicating a coherent dextral rotation of about 30° since 4 Ma. The nature of the transition from translation to rotation of the overthrust crust is described by *Little and Roberts* [1997] on the basis of the rotated structural fabric of the basement rocks. The amount of dextral slip on the major strike-slip faults decreases toward the edge of the rotated block in the manner envisaged by *Lamb and Bibby* [1989]. Pre-Pliocene rotation of about 90° seen in the paleomagnetic declinations of older rocks points to very substantial rotations in at least part of the obducted crust [*Vickery and Lamb*, 1995].

3.2.1.7. Subduction of lower lithosphere: Lower continental lithosphere must separate and move downward under the edge of the NW dipping, subducted Pacific plate, while the upper crust is being obducted onto it. The subduction of the lower lithosphere is shown by NE dipping earthquakes in Figure 11 [from *Anderson et al.*, 1993] and is illustrated in Figure 10b. The deformation associated with this NE directed collision with the subducted plate can be identified up to 130 km south of Kaikoura into north Canterbury where the lower crust and mantle first start to dip northward [*Reyners and Cowan*, 1993]. There northward verging thrusts and

folds of Pliocene–Quaternary age in north Canterbury [*Nicol et al.*, 1994], as well as offshore [*Barnes*, 1996], result in northward crustal thickening and increasing separation of upper and lower lithosphere. The northward verging fold and thrust belt marks the southern limit of a "Marlborough overthrust complex" which, though structurally associated with the southeast verging Hikurangi subduction complex, is a distinct major structural feature of the northern South Island related to the NE transport of continental lithosphere away from the collision zone.

3.2.1.8. Crustal thickening and erosion: Uplift of the Kaikoura Ranges along reverse faults [*Lamb and Bibby*, 1989] show that some shortening across the plate boundary zone is accommodated by crustal thickening, but most is taken up by the transport of crust away from the collision along the dextral strike-slip faults to overthrust the subducted oceanic lithosphere to the northeast. The transport is achieved by two mechanisms: the rotation of tabular blocks of crust between synthetic dextral faults and antithetic sinistral faults and their sideways expulsion over the adjacent subducted oceanic lithosphere. Erosion is not the dominant mechanism as it is in the central part of the South Island. In the north, crust is mostly conserved and has merely been pushed sideways away from the collision toward the adjacent subduction zone.

The division between conservative mechanisms of the north and the erosional destruction of continental crust of the central region is gradational, and an increasing proportion of excess crust is accommodated by rock uplift along the Southern Alps and erosion with distance southward from the Wairau fault.

3.2.2. Deformation west of the Alpine and Wairau faults. The distinctive tectonic feature on the western side of the northern segment of the plate boundary is the reactivation of Late Cretaceous and early Cenozoic extensional faults in the Miocene as reverse faults [*Gage*, 1952]. Inversion of earlier basins is pervasive throughout the region and northward into the offshore Taranaki basin. The movement occurred mainly in Pliocene–Quaternary time [*Nathan et al.*, 1986]. Miocene reverse faults that resulted in the uplift of many of the main ranges of northwest South Island are no longer active, though there exists a belt of seismicity extending northward through the northwesternmost South Island within which three of the largest earthquakes of the twentieth century have occurred. Despite this recently high level of activity, the deformation is at a low level on a longer timescale [*Holt and Haines*, 1995].

Kamp et al. [1992] suggest from their fission track studies that denudation of several kilometers of crust occurred in Westland adjacent to the Alpine fault during late Miocene to Recent time, with the amount of rock uplift increasing northward from some 3 km in the south to as much as 12 km in the north.

The Alpine fault bends sharply through an inflection of about 20 km in the northern segment of the plate boundary. The Alpine fault is considered [*Walcott*, 1978; *Anderson et al.*, 1993] to have once been straight, continuing along the Wairau fault and Cook Strait to the Hikurangi subduction zone, and the bend is thought to have been caused by differential shortening of some 20 km in northwest South Island during the late Miocene and Pliocene–Quaternary (shown stippled in the top inset in Figure 8). If so, the steepest gradient in the differential shortening would be immediately west of the bend. Along the north coast of the South Island there are a number of NE trending reverse faults and ENE trending dextral faults involving fault slivers of Oligocene sediments [*Mortimer*, 1993]. The reconstruction in the top inset of Figure 8 accounts for the consequent NW-SE shortening by stretching the north coast of the South Island through 30%, but the actual amount and age are unknown.

3.3. Central Segment

From 12 to 6 Ma the amount of convergence between the plates was small, only about 15 km in the central parts of the Alpine fault, or less than one fifth of the total. By far the greatest shortening occurred in Pliocene–Quaternary times. The area of crust lost since 6.4 Ma is about 27,000 km^2 (300 × 90 km), and taking the crust to be originally 25 km thick, a volume of 0.6×10^6 km^3 has been lost from the plate boundary zone. A root under the Southern Alps presumably developed early in the period of compression together with the rise of the Southern Alps. Its volume is roughly estimated to be 0.25×10^6 km^3 taking its dimensions to be length of 300 km, width of 85 km and increased depth over normal crust of 20 km. The last is not well known, but it is unlikely to be more than 25 km, and from gravity modeling it is estimated to be 10 to 15 km [*Stern*, 1995]. Most of the accommodation is therefore by erosion, and around 0.35×10^6 km^3 of sediment is expected to have come from the eroding Southern Alps during the Pliocene–Quaternary.

Sediment accumulated largely along the west coast of both South and North Islands in a thick (3–4 km), prograding wedge of clastic sediments some 50–100 km wide and 700 km long forming the characteristic "prograding clinoforms" of the Westland basin [*Sutherland*, 1996] and "Giant Foreset Beds" of the Taranaki basins accounting for 0.2×10^6 km^3 (700 × 80 × 3.5). Sediment carried great distances east of the eroding Southern Alps to the Bounty Fan (20,000 km^2 in area, about 2 km thick) and northward by the boundary current to be deposited in the Hikurangi and Kermadec Trenches [*Carter and McCave*, 1994] account for about 0.1×10^6 km^3. The remaining 0.05×10^6 km^3 may be on the shelf and platform in east central South Island or carried even farther afield by currents in the Tasman Sea.

3.3.1. West of the Alpine fault. Today, the central parts of the west coast are stable and part of the Australian plate, and most deformation occurs at or east of the Alpine fault. Numerous large earthquakes occur

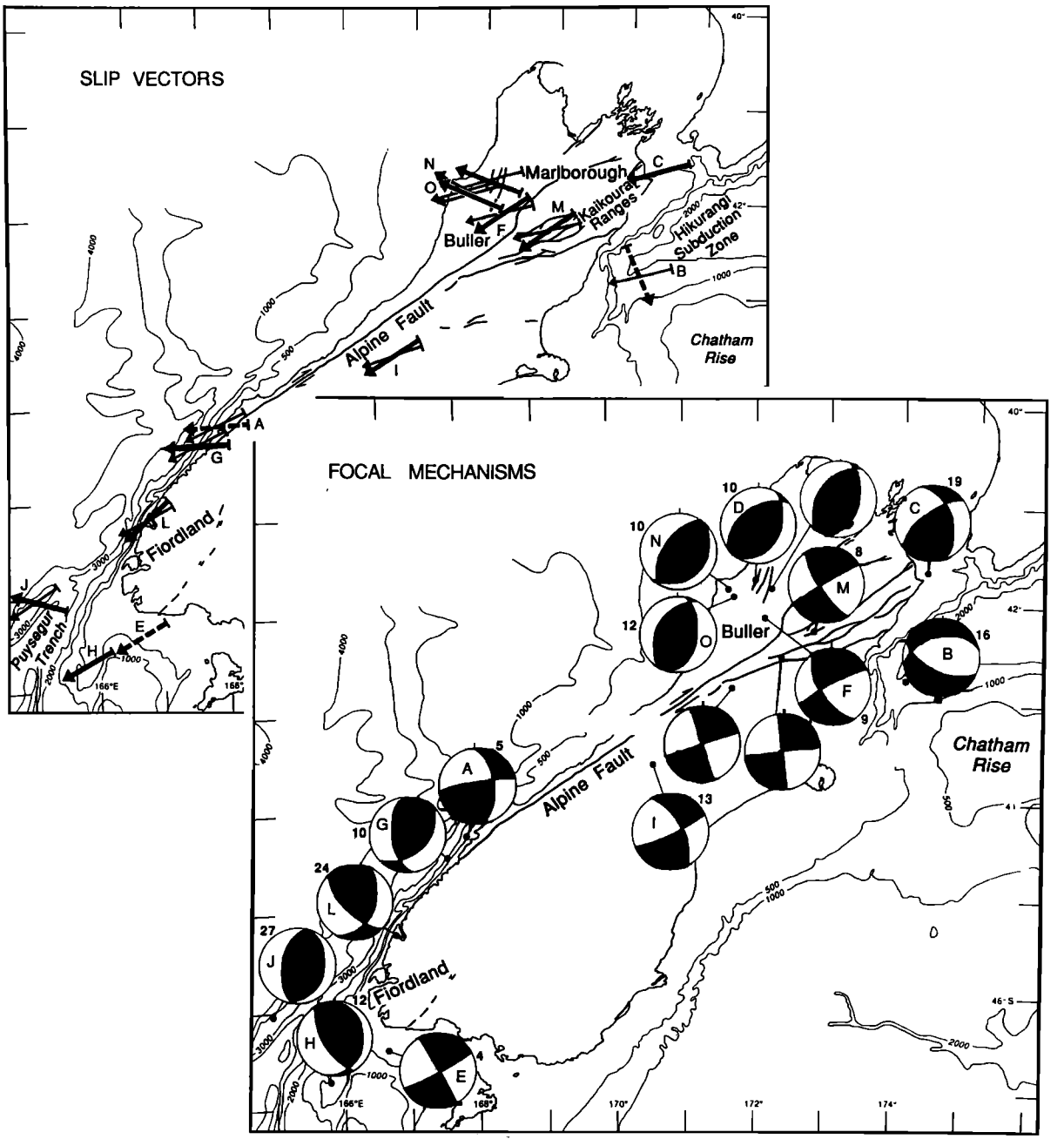

Figure 12. Slip directions and source mechanisms of large recent earthquakes from *Anderson et al.* [1993]. Earthquake depth in kilometers is shown adjacent to the source mechanism.

on the southernmost west coast around and south of Jackson Bay (Figure 13). All are thrusts with slip vectors (Figure 12) in the direction of relative plate motion [*Anderson et al.*, 1993] and presumably are due to oblique slip on the Alpine fault where Pacific plate continental crust impacts subducted oceanic lithosphere. In central parts of the west coast of the South Island, however, there is currently little seismic activity, and flat-lying Pliocene sediments of the Westland basin beyond the coast indicate little deformation there in the last 3 Myr apart from a regional subsidence. Active deformation continues in the northern and southern west coast as well as within 5 km of the central part of the Alpine fault.

3.3.1.1. South Westland fault zone: Earlier, in the late Miocene, deformation west of the Alpine fault was more extensive than it is today, and a major, steeply dipping dip-slip fault, the South Westland fault zone (SWFZ) developed approximately along the present coastline some 20 km west of the Alpine fault. Near Jackson Bay, in southern Westland, southeast dipping reverse faults of the SWFZ became active in the mid-Miocene [*Nathan*, 1978; *Sutherland*, 1996]. Dip-slip displacement of around 3.5 km resulted in the formation of

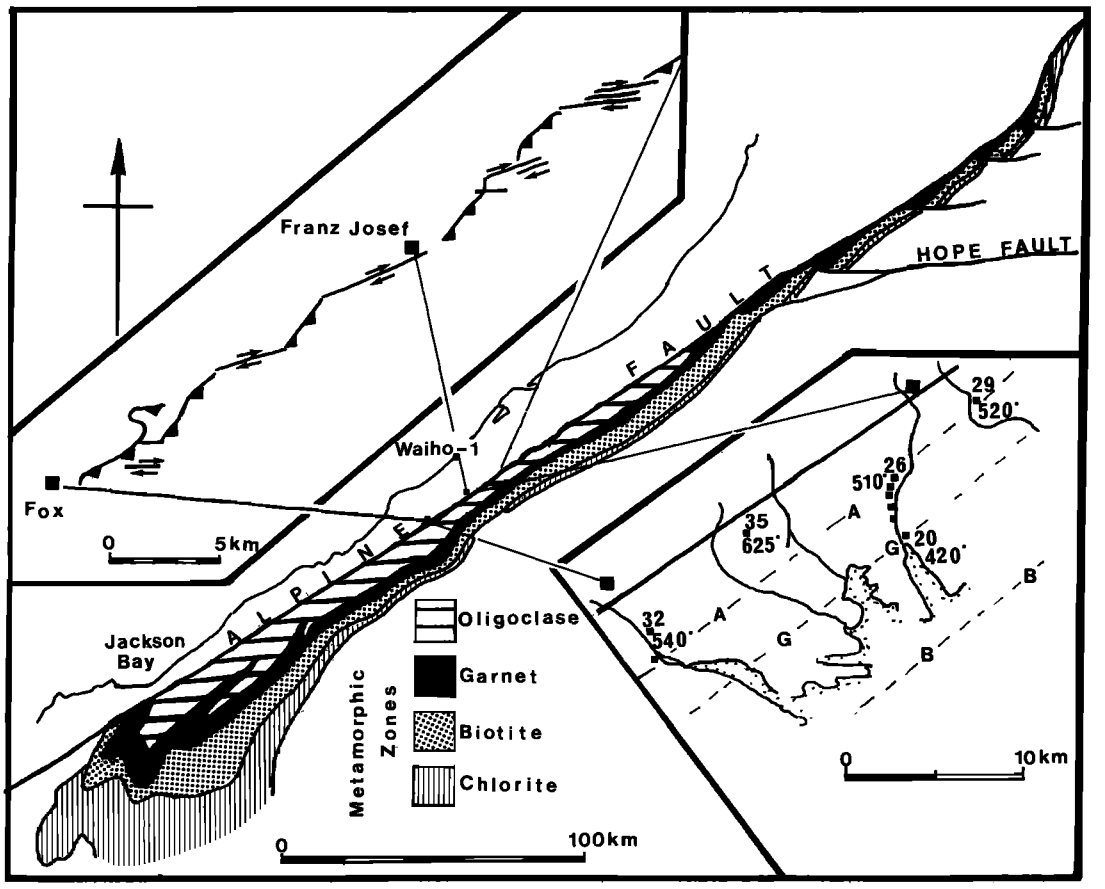

Figure 13. Central Alpine fault and Southern Alps. At small scale the Alpine fault is straight and trends 55° and bounds high grade schists of the Southern Alps. At large scale (top left inset) the Alpine fault is complex with short thrust segments linked by transfer faults [from *Norris and Cooper*, 1995]. The bottom right inset of the Franz Josef–Fox area shows locations of samples with their estimated depth (in kilometers) and temperature of metamorphism (in degrees Celsius) [from *Grapes*, 1995].

a coastal monocline. Bathyal clastic sediments conformably overlie shallow-water Oligocene limestones, which were deposited on an unconformity cut on Paleozoic and older crystalline and sedimentary rocks that form the basement of Westland and the Challenger Plateau. So evidently, through Oligocene and early Miocene times the basement subsided, with sedimentation failing to keep up with the subsidence until at the end of the Miocene, the ocean floor lay at depths of ~1–2 km like the rest of the Challenger Plateau today [*Wood*, 1991]. The onset of rapid compression in latest Miocene resulted in rapid deposition of clastic sediments derived from the eroding Southern Alps and continued slip on the SWFZ. Basin infilling from the coast westward occurred during the Pliocene through northwestward prograding wedges of clastics. A borehole, Waiho-1 (Figure 13), located a few kilometers northwest of the SWFZ, yields the history of deposition adjacent to the Southern Alps [*Sutherland*, 1996]. The earliest sediments are Oligocene limestones overlain by bathyal Miocene clastic sediments. Sedimentation rates were very low up until the mid-Miocene, around 12 Ma, when clastic sediments first appear in any quantity. About 1000 m of sediments older than 6.4 Ma occur in Waiho-1. The bulk of the sediments, 2500 m, are younger. Rapid accumulation of sediments and erosion of the source region commenced in the late Miocene (the precise timing is not resolvable), in general agreement with plate tectonic history. Interestingly, sedimentation rates on the west coast are low throughout the early Miocene, a period of particularly rapid sedimentation on the east coast of the North Island and the northeastern South Island. Oligoclase-garnet zone schist typical of the rocks now outcropping along the eastern side of the Alpine fault appears around 3 Ma.

The South Westland fault zone continues northward approximately along the present coastline, producing a step of several kilometers in depth to basement and defining the southeastern edge of Westland basin. *Kamp et al.* [1992] identify the Westland basin as a foreland basin produced by flexural downwarping through thrusting at is southeastern margin. *Sutherland* [1996] argues that the basin formed largely by subsidence under the load of Pliocene–Quaternary sediments. At issue here is the cause of the initial subsidence that has been isostatically amplified by sedimentation. As the Waiho-1 bore-

hole indicates, there was already a deep, unfilled depression by the time rapid sedimentation commenced in the late Miocene, and the question is whether that depression is large enough in itself to account for the present thickness of Pliocene–Quaternary sediments without the need for thrusting at the margin. Isostatic subsidence due to the load of Pliocene–Quaternary sediment would be 2.3 times the initial depth of water, if locally compensated, and less than that if the lithosphere partly supports the load. For local compensation, take the initial depth of water to be H and the thickness of the accumulated sediments of density 2.3 Mg/m^3 to be X, then $X = 2.3\ H$. Since X is close to 3.5 km, H would be around 1500 m, about the average depth of the Challenger Plateau west of the influence of Pliocene–Quaternary sedimentation. The movement on the SWFZ is therefore largely an isostatic response to the sedimentary load, and the SWFZ is primarily due not to thrusting but to isostatic amplification of a preexisting depression. The Westland basin and the Pliocene–Quaternary Taranaki basin farther north are better described as prograding deltaic basins like those at passive margins where there is a large sediment source rather than as a foreland basin [*Beaumont et al.*, 1996] produced by thrusting at the margin. The contribution to basin subsidence by plate margin thrusting is likely to be small, if it occurs at all.

3.3.1.2. Low-angle basement thrusts west of the Alpine fault: In central Westland, low-angle thrusts within 5 km of the Alpine fault carry basement over Miocene sediments and, in places, Pleistocene gravels [*Rattenbury*, 1986, 1987]. The stack of thrusts splays westward from the Alpine fault [*Rattenbury*, 1986]. The present-day dip of the Alpine fault is around 50°. When motion on the fault was purely strike-slip, it seems likely that the fault was vertical. Thus the low-angle thrusts can be understood as resulting from the shallowing of dip of the Alpine fault as it evolved from a vertical strike-slip fault in Miocene time to the southeastward dipping oblique slip fault of today [*Sibson et al.*, 1979]. Although some of the thrusting is recent, zircon fission track studies suggest that the uplift and denudation associated with the emplacement of the thrust sheets occurred about 9 Ma [*White and Green*, 1986].

3.3.2. The Alpine fault. At the northern end of the Fiordland block the rate of slip on the Alpine fault is about equal to that of relative plate motion. There *Wellman and Wilson* [1964] calculated from offset moraines a horizontal slip rate of 25 mm/yr, a result confirmed in detailed work on several offset features by *Sutherland and Norris* [1995]. Uncertainties in age or the geometry of offset leave uncertainties in slip rates of about 6 mm/yr.

In the central segment the Alpine fault appears to be very straight and sharply defined on small-scale maps. *Norris et al.* [1990] and *Norris and Cooper* [1995] have described the shallow structure of the Alpine fault and show it to be more complex with short NNE-SSW thrusts carrying mylonites and schist over Pleistocene gravels linked by ENE-WSW to ESE-WNW transfer faults (Figure 13). The rate of thrusting is not well determined but is estimated to be 5–15 mm/yr. Slip rates parallel to the 55° trend of the Alpine fault are at least 25 mm/yr. *Berryman et al.* [1992] also estimate rates of slip at a large fraction of the plate motion rate.

3.3.2.1. Direction of plate motion: The direction of relative plate motion near Franz Josef is 73°, and it is frequently stated that directional indicators of striations on transfer faults and stretching lineations in mylonites are parallel to plate motion. This is incorrect. The direction of motion revealed by the strike of the transfer faults is systematically clockwise by some 20°. The top left inset in Figure 13, modified from *Norris and Cooper* [1995], shows the transfer faults in central Alpine fault to be about 85°. Striations on the transfer faults range in azimuth from 65° to 120°. A systematic clockwise swing in direction is also seen in the orientation of the stretching lineations in the mylonites of the Alpine fault (Figure 14). Described by *Sibson et al.* [1979], the stretching lineations mostly point 90° with some particularly well developed and consistent sets at 120°. There is scatter in the directions, but none trend at an azimuth of less than 70°. The average for a large part of the central Alpine fault is about 100°. The plunge of the lineations varies from 17° to 52° degrees, with some of the best determined being the higher values. A slip vector of 73° requires the ratio of motions normal and parallel to the Alpine fault trend to be the same as those for the overall plate motion, and a clockwise swing in the slip vector requires a higher proportion of normal to parallel motion. Where a slip vector direction of 90° (=55° + 35°) occurs, the ratio of normal to parallel motion would be 0.7.

3.3.2.2. Drag on the Alpine fault: Some freshly glaciated surfaces at distances of ~3–5 km from the Alpine fault show displacements by slip on schistosity planes like those at the fault itself: up to the east, dextral offset with a principal axis of shortening of 126° azimuth similar to that of earthquakes and geodetic strain and to the long-term slip on the Alpine fault [*J. Adams*, 1979; *Norris and Cooper*, 1986]. J. Adams estimated the vertical strain by summing vertical displacements across a 100-m-wide outcrop and obtained a value of 3×10^{-3}. The outcrop was deglaciated some 20 years before, and assuming the displacement commenced then, he obtained an uplift rate of 17 mm/yr across the outcrop. *Norris and Cooper* [1986] reexamined the outcrop and observed no change in displacement in the 6 years since the first observation. It is possible therefore that the observed displacements accumulated over a longer time interval or that they developed episodically. Their existence may point more toward short-term high-stress conditions near the culmination of the earthquake cycle than toward a sustained deformation. Certainly when the Alpine fault is modeled as a thrust locked at depths of around 5 km, the most intense strains and stresses at

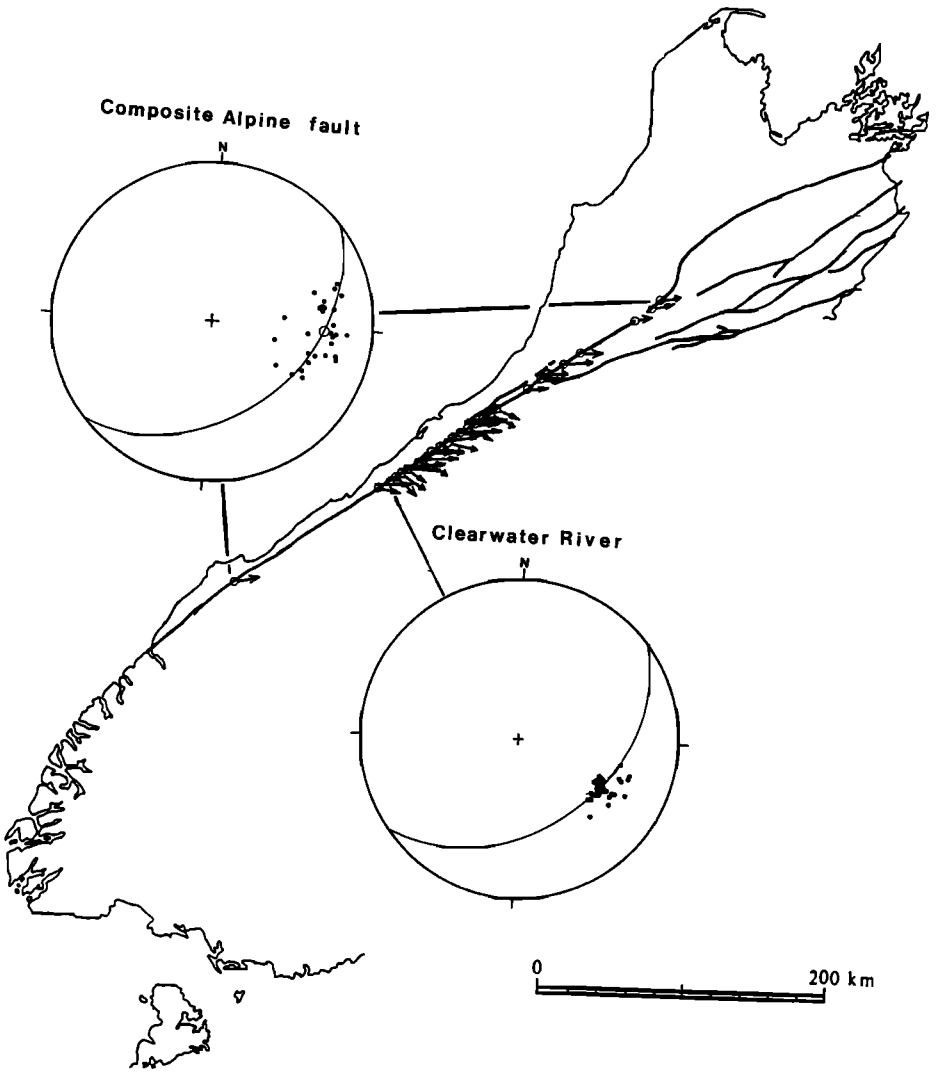

Figure 14. Stretching lineation directions from *Sibson et al.* [1979]. The mean direction is about 80°, but there is a clear difference between those in the Franz Josef–Fox area and those to the north and south. An explanation is that the ratio of the normal component of motion to the strike-slip component is greater in the center than at the ends of the Alpine fault. The mean direction of 120° in the Franz Josef area requires a shortening rate twice the value of the strike-slip rate, whereas at the northern and southern ends the direction of motion is close to the relative plate motion with a normal:strike-slip ratio of 0.3.

the surface occur at about the distance from the Alpine fault that the displacements are found.

Whatever the cause of these displacements, they point toward the accommodation of some of the deformation between the plates at least 5 km southeast of the Alpine fault. The sense of displacement is the same as that on the Alpine fault, so these displacements would lessen the amount on the Alpine fault. J. Adams [1979] referred to the off-fault accommodation of strain as fault drag, but it would be so only if it were a large fraction of the total. A strain of 3×10^{-3} indicates that a significant proportion of the deformation could be taken up off-fault. However, not knowing the time over which the strain accumulated prevents drawing any definite conclusions.

3.3.3. Rock uplift, exhumation, denudation, and the thermal structure of the Southern Alps. The increase in metamorphic grade from eastern South Island westward to the Alpine Fault (Figure 13) has long been held [*Suggate*, 1963] to be due to an increase in depth of erosion with some 20–30 km of exhumation adjacent to the fault in the Fox–Franz Josef Glacier area and somewhat less than that to the north and south. Potassium-argon studies [*Mason*, 1962; *Sheppard et al.*, 1975; *C. Adams*, 1979, 1981; *Adams and Gabites*, 1985] established that rocks within 12 km of the Alpine fault have K-Ar ages less than 10 Ma with apparent age progressively increasing eastward to Jurassic–Early Cretaceous ages in greywackes far from the fault.

3.3.3.1. Fission track studies: *Kamp et al.* [1989] show that fission track ages determined from apatite and zircon are very young near the Alpine fault and increase systematically with distance eastward, just as the K-Ar ages do. In transects normal to the Alpine fault, apatite ages are zero out to a distance of around 30 km after

which ages increase to about 40 Ma. Zircon fission track ages are also low near the fault, but around 10 km they increase sharply to Mesozoic ages. The point in the transect where the age for each mineral first start to increase is taken to mark the base of an exhumed partial annealing zone for that mineral.

Annealing in apatite and zircon is manifest in reduced track length and track density and is a time and temperature dependent process. At very high temperatures, tracks are annealed as fast as they are formed, but when the temperature drops below a value characteristic of the mineral, tracks survive. Even then they anneal slowly with time, and only when the temperature drops sufficiently far do all tracks survive unaltered over geological time. This lower temperature is sometimes referred to as the closure temperature of the mineral. Apatite samples collected from deep boreholes where the ambient temperature is above the closure temperature show track densities, and hence apparent ages, less than those for rocks at shallower depths in the hole. The apparent age decreases progressively with increasing depth and temperature until it becomes zero. This depth is inferred to be the base of the partial annealing zone.

Tippet and Kamp [1993a, b] report a number of additional fission track studies east of the Alpine fault and map the outcrop of the base of apatite and zircon partial annealing zones (PAZ). By assuming an initial geothermal gradient and inferring the temperature of the PAZ from elsewhere, they estimate the depth at which the rocks initially lay and hence the uplift that has occurred during the collision. There are two problems with their analysis: the temperature, and hence the depth, inferred for the base of the zircon partial annealing zone, and the implicit model from which rates and amount of uplift are inferred.

The temperature at the base of the apatite PAZ is estimated from samples collected from boreholes in the Otway basin. There, for samples that have been maintained at high temperatures for geological time periods, it is 125°C, and the apatite closure temperature is around 60°C [*Tippet and Kamp*, 1993a].

For zircon the temperature at the top of the PAZ exceeds 200°C on a geological timescale of several million years in zircons from a deep borehole in the Vienna basin [*Tagami et al.*, 1996], consistent with the closure temperature estimated by *Hurford* [1988] of 240° ± 50°C obtained from cooling and uplift patterns in the Lepontine Alps by extrapolation between K-Ar and Rb-Sr mica ages and apatite fission track age. However, there is no direct measurement of the temperature of the base of the zircon PAZ on a geological timescale, and estimates vary widely. *Kamp et al.* [1989] and *Tippet and Kamp* [1993a, b] assume a temperature of 265°C, very close to the closure temperature of *Hurford* [1988]. This appears to be much too low. An experimental study by *Yamada et al.* [1995] relates variation in normalized mean track length r of confined lengths of spontaneous fission tracks in zircon to the time and temperature of annealing. The experimental times and temperatures are extrapolated on an Arrhenius diagram to geological time periods. For a time of 50 Ma, which is appropriate for those rocks in the Southern Alps that have attained long-term equilibrium, estimates for the partial annealing zone temperatures in their preferred model are 170°C for the low-temperature bound (i.e., the top of the PAZ), defined for $r = 0.95$, and 390°C for the high-temperature bound (base of the PAZ), defined for $r = 0.4$. The definition of *Tippet and Kamp* [1993a] for the base of the zircon PAZ in terms of age is not the same as that for the experimental study, which is in terms of track length distribution, and there are insufficient published data to establish a relationship between one definition and the other. However, it is apparent that the temperature at the base of the PAZ is not well determined. It is likely to be greater than 265°C and may be as much as 390°C.

In their analysis of the fission track ages and outcrop patterns of the partial annealing zone, Tippet and Kamp derive and map a number of parameters: "rock uplift," "mean uplift rate," and "uplift age." The meaning of these parameters is not obvious. Their mean uplift rate map [*Tippet and Kamp*, 1993a, Figure 13] differs considerably from the uplift rate maps of *Wellman* [1979] or *Adams* [1980] with values about 4 times smaller. Whereas the rates estimated by Wellman and Adams are sufficient to provide a flux of material through the surface to balance crustal convergence, this is not so for Tippet and Kamp's mean uplift rate. Wellman's and Tippet and Kamp's uplift rates in profile are shown in Figure 15. The amount of rock uplift is similarly much smaller than the amount of crust lost since 6.4 Ma. From their map of total uplift [*Tippet and Kamp*, 1993a, Figure 10] it is easy to compute the total volume of rock that would have been eroded. It is 0.1×10^6 km^3 compared with the 0.6×10^6 km^3 given earlier.

The principal difficulty with their analysis is that it is one dimensional for what is inherently a two-dimensional problem: with a total shortening of 90 km there is a very much larger component of motion parallel to the isotherms than perpendicular to them, and the isotherms are not everywhere parallel to the surface.

A more appropriate, two-dimensional, model is illustrated in Figure 15 based on a suggestion by *Wellman* [1979]. Pacific lithosphere consisting of 25-km-thick crust resting on old oceanic lithosphere, converges on the Alpine fault at 13 mm/yr. At a distance of 100 km from the Alpine fault, the oceanic lithosphere separates and sinks into the asthenosphere, and the crust is deflected upward to be eroded at the surface. A root of lower crustal material is assumed to have formed early during convergence and now supports topography of about 3 km at the Main Divide. The total area of rock removed by erosion or accumulated as a root is 90×25 km. The velocity of rock everywhere is 13 mm/yr, and the vector is steeper at the Alpine fault (60° in this model), progressively less so eastward to be less than 1 mm/yr at distances greater than 65 km from the Alpine fault. The

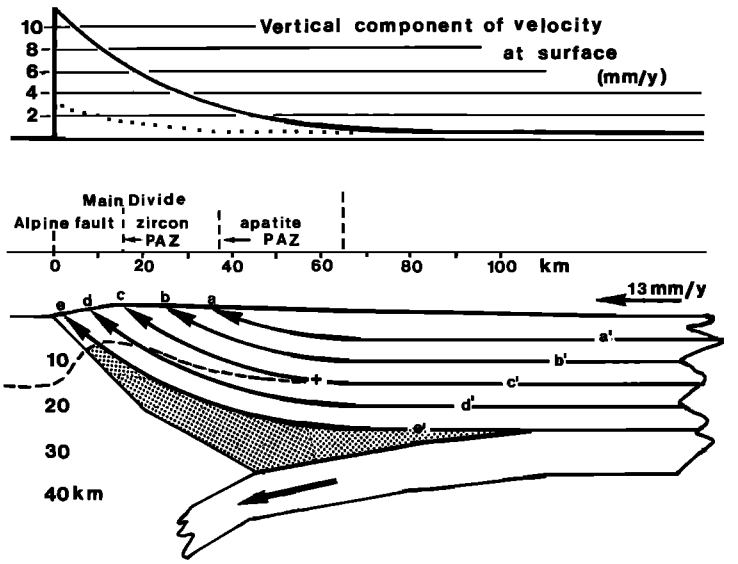

Figure 15. Cross section illustrating the presumed shortening process occurring in the Southern Alps. Crust 25 km thick is deflected upward to erode at the surface. A crustal root formed early in the collision is shown stippled and supports topography reaching some 3 km at the Main Divide. There has been 90 km of shortening, and samples today located on the surface at *a* through *e* originated at *a'* through *e'* at increasing depths of 5–25 km. The vertical component of velocity at the surface is shown in the top diagram as the heavy solid line and is close to that given by *Wellman* [1979, Figure 1]. The uplift curve from *Tippet and Kamp* [1993a, Figure 10] (dotted) is also shown. The positions at which rocks originally at temperatures of 375°C and 125°C, outcrop, taking the initial thermal gradient to be 25°C/km, are shown as *c* and *a* and are close to the observed outcrop of the base of the partial annealing zones of zircon and apatite (arrows). The dashed line in the bottom diagram represents the present position of the 375°C isotherm advectively deflected upward. The apparent age of the sample at *c* will be related to the time spent within the partial annealing zone and is related to path length from the surface to the cross.

inclination of the velocity vector can be estimated from the horizontal width at the surface of zones whose initial vertical separation is known. Thus the 20-km horizontal separation between the base of the apatite and zircon PAZs, were initially separated by 10 km in the model, requires an inclination of about 30° at that part of the profile. The vertical component of velocity at the surface is shown in the upper graph and is presumed to follow an exponential curve $W_0 e^{-\alpha x}$, where W_0 is the uplift rate at the Alpine fault and x is the distance from the fault. Assuming erosion to now balance convergence, α must equal W_0 divided by the product of the convergence rate (13 mm/yr) and crustal thickness (25 km). W_0 is taken to be 11.5 mm/yr, and the curve closely corresponds to the uplift rates estimated by *Wellman* [1979, Figure 1]. Samples *a* through *e* at the surface today would have been located at *a'* through *e'* at depths of 5 to 25 km at the start of convergence, and taking the geothermal gradient to be 25°C, *a'* would lie at the base of the apatite PAZ (125°C) and *c'* would be near the base of the zircon PAZ (375°C). The model fits the fission track data well. The base of the apatite PAZ outcrops at *a*, about 35 km from the Alpine fault, just as *Tippet and Kamp* [1993, Figure 3] show. The base of the zircon PAZ lies a variable distance from the Alpine fault of 25 km near Haast and only 7 km at the northern end of the central segment of the plate boundary. Mostly, however, it outcrops at *c*, 15 km from the fault, as is shown in the model.

Using the two-dimensional model, the meaning of the parameters used by *Tippet and Kamp* [1993] can be deduced. The parameter "rock uplift" is the distance from the surface to the initial depth; i.e., at *a* the rock uplift is 5 km (the distance from *a'* to the surface), while at *c* it is 15 km (the distance from *c'* to the surface). This is not the same as the amount of rock removed at *a* or *c*, which is ~90 km in both cases. The parameter "age of uplift" is determined from the "weighted mean of reset and annealing zone age pair in each transect" [*Tippet and Kamp*, 1993a, p. 16,138]. In the two-dimensional model this represents the age of the sample at *c*, which first began to cool from its initial temperature at some position such as that marked with the cross. The path length is 50 km from the cross to the surface at *c*, and with a velocity of 13 mm/yr an apparent track age for *c* would be 4 Ma. This is similar to the ages given by *Tippet and Kamp* [1993a, Figure 12]. The time taken in transport from the position *c'* to the position of the cross is not included in the age of uplift, and hence age of uplift is not equivalent to the age at which compression, or even rapid rock uplift, commenced. The parameter "mean uplift rate" is determined by dividing rock uplift by age of uplift and is hence an average vertical speed at which a sample moves from its initial depth to the surface. As uplift rate is likely to be highly nonlinear with time, very much slower in the beginning than at the end, the mean uplift rate is not a useful parameter. It is certainly not equivalent to the vertical component of velocity at the surface, which is what others mean by uplift rate.

The uncertainty in the temperature of the base of the zircon PAZ currently limits the value of fission track studies in estimating the temperature-depth structure. However, these studies clearly have great potential value. *Kamp et al.* [1989], and subsequent authors, have demonstrated that the exhumed partial annealing zones of apatite and zircon can be mapped in a coherent way within the Southern Alps. While the outcrop pattern of the PAZs is likely to be related to the temperature,

structure, and deformation history, estimates of the temperature and depth of the PAZ boundaries need to be further constrained by experiment and observation.

3.3.3.2. Definitions: Two-dimensional deformation requires some modification of the definitions introduced by *Molnar and England* [1990] for one-dimensional erosion and uplift. As with the one-dimensional case, rock uplift is the vertical component of the displacement vector relative to sea level, but in two dimensions it may vary in horizontal position and depth. Surface uplift remains the vertical component of the Earth's surface displacement relative to sea level, and exhumation, which in one dimension is the difference between rock uplift and surface uplift and so is the thickness of rock removed at the surface, is now better defined as the net vertical displacement relative to sea level. In two dimensions the amount of rock removed by erosion at a point on the Earth's surface may be vastly greater than the exhumation and is better referred to as denudation. Thus in Figure 15 a rock at *c* has been exhumed from a depth of 15 km by denudation of some 90 km.

3.3.3.3. Rock uplift rate: Considering how important they are in modeling deformation [*Beaumont et al.*, 1996] and thermal structure [*Allis and Shi*, 1995] there is remarkably little hard, direct information on rates of rock uplift anywhere near the Alpine fault. There have been no geodetic measurements of uplift rate to date. *Adams* [1980] and *Wellman* [1979] summarize the information available until 1980. *Adams* [1980] lists a number of observations that can be reasonably interpreted as indicating uplift rates immediately southeast of the Alpine fault of around 11 mm/yr at the Paringa River and 12 mm/yr at the Wanganui River, locations about 50 km southwest and northeast of the Waiho River, respectively. Both are open to alternative explanations and are contentious. In modeling uplift rates across the Southern Alps, *Adams* [1980] derived the variation in uplift rate with distance by requiring the integral of the uplift curve to equal the convergence rate.

For his map, which has been the principal source of uplift rate data in most work for the last several years, *Wellman* [1979] measured and correlated tilted shorelines on late Quaternary lakes southeast of the Southern Alps. He inferred the tilt to be relatively simple in pattern and to increase exponentially toward the Southern Alps, doubling every 7–8 km. By integrating the exponential relationship, he deduced uplift rates of 0.5 mm/yr, increasing to 2 mm/yr some 55 km southeast of the Alpine fault. For the crest and western slopes of the Southern Alps he assumed a relation between summit heights, rainfall, and uplift. Northwest of the crest of the Southern Alps he summarized a variety of information on river aggradation terraces and inferred the highest rates, 17 mm/yr, to occur 5 km southeast of the Alpine fault.

More recently, *Cooper and Bishop* [1979] identified a prominent terrace at 1450 m and another at 960 m southeast of the Alpine fault near Haast in south Westland as marine terraces. *Adams* [1980] presumed these to be penultimate and last interglacial terraces and calculated uplift rates of 6 and 8 mm/yr. *Bull and Cooper* [1986], in a rather more developed analysis, identify further notched ridge crests and flat summits on the steep western ridges descending to the Alpine fault from the Southern Alps as a sequence of marine terraces. The ages of the terraces are inferred by correlating their relative height sequence with the Huon Peninsula sequence of marine shorelines. Rates of uplift in the central Alpine fault are estimated to be about 8 mm/yr for the last 135 kyr and somewhat less earlier. The identification of the notches as marine terraces is contentious [*Ward*, 1988], and their inferred ages are model dependent and await confirmation by direct dating.

3.3.3.4. Lower lithosphere subduction: Lower lithosphere subduction must occur merely to accommodate the consumption of the lithosphere, as was pointed out clearly by *Wellman* [1979]. Where the lithosphere splits, either in vertical section or in horizontal location, into that part which is eventually uplifted and eroded and that part which sinks into the asthenosphere is not known. Small, intermediate-depth earthquakes down to depths of 80 km under the Southern Alps [*Reyners*, 1993] presumably arise in the subducted lower lithosphere. The subduction of lower lithosphere has important consequences for the thermal structure in that isotherms are carried down and thus flatten the thermal gradient in the region where the separation occurs between uplifting and subducting lithosphere.

3.3.3.5. Heat flow and thermal structure: The only direct measurement of heat flow is reported by *Allis and Shi* [1996]. A 220-m drill hole 4 km SE of the Alpine fault in the Waiho valley within the outcrop of high-grade schists gave a gradient, after a 40% correction for topography, of 60° ± 15°C/km and heat flow of 190 ± mW/m^2. All other cited information on the thermal structure in the vicinity of the Alpine fault is based on estimates from thermal modeling, based on rates of uplift and a presumed geothermal gradient, or fluid inclusion and fission track studies. Fission track studies are discussed in a separate section below.

Holm et al. [1989] report very high temperatures at shallow depths inferred from studies of fluid inclusions in veins of the high-grade schists of the Waiho valley. Depth-temperature estimates of 3 km at 285°C, 6–8 km at 310°–350°C, and 15–20 km at 400°–450°C are given. The brittle-ductile transition is estimated to occur at depths of 5–6 km. *Jenkins et al.* [1994] studied calcite and quartz veins developed in steeply dipping fissures within the high-grade schists and argue, using stable isotopes, that they were deposited from mainly meteoric water under hydrostatic pressures down to the brittle-ductile transition. Pressure estimates obtained from fluid inclusions in fissure veins of quartz and calcite were in the range 200–400 bars for temperatures estimated to be 200°–350°C. Again, this work pointed to very high temperatures at shallow depths.

Allis and Shi [1995] and *Shi et al.* [1996] model the evolution of the thermal regime in the Southern Alps since 10 Ma with boundary conditions based on (1) convergence of 70 km at rates increasing linearly from 5 Ma to a present rate of 20 mm/yr, and (2) rock uplift and erosion rate of the upper surface of the profile taken from the *Wellman* [1979] uplift map. Insofar as these two conditions do not balance, so that erosion fails to keep up with the increasing rate of convergence, there is a net accumulation of crust at depth as crustal thickening. The main feature of their model is that geotherms are carried both downward with the sinking of the lower part of the lithosphere and the accumulation of crust at depth as well as upward near the Alpine fault so that the gradient becomes quite flat near the base of the crust. The thermal structure fits the observed thermal gradient well. Temperature estimates inferred by *Kamp and Tippet* [1993] from reset ages in fission track and K/Ar studies also fit this model. The model does not fit the data of *Holm et al.* [1989] nor those of *Jenkins et al.* [1994]. *Allis and Shi* [1995] argue that fluid inclusion depths may be due to episodic periods of lowered pressure following earthquakes. It is clear, however, from the *Shi et al.* [1996] modeling that a shift in boundary conditions, the speed of transport of lower crust toward the surface, or the initial temperature profile could result in higher temperatures being carried upward, resulting in an elevated rather than a depressed brittle-ductile transition.

3.3.4. Intrusion of the lower crust along the Alpine fault. The Fox–Franz Josef Glacier area, lying near the middle of the Alpine fault, is unusual in that the width of the high-grade schist is about half that to the north and south; at Haast in the south it is about 15 km, and at Wanganui River in the north it is ~10 km. While this area is one of the most intensively studied, it may not be typical of elsewhere on the Alpine fault. However, it displays features that point to an important structural process that develops during compression of continental crust: intrusion of the ductile lower crust upward into the brittle upper crust (Figure 16).

3.3.4.1. A highly condensed lower crustal section: Pressure-temperature (*P-T*) estimates of 10 samples from the high-grade schist section near the Franz Josef–Fox Glacier region are reported by *Grapes and Watanabe* [1992]. All rocks come from a 5-km-thick section immediately east of the Alpine fault (Figure 13, bottom right inset) in which zircon fission track and K-Ar ages are less than 5 Ma. *P-T* conditions are estimated using garnet-biotite Fe-Mg exchange geothermometry and garnet-biotite-muscovite-plagioclase geobarometry. Maximum temperature and pressure conditions of 625°C and 9.2 kbar, for the sample closest to the Alpine fault, are consistent with the high-pressure anatexis shown by mica pegmatites within the schists south of Fox Glacier. Assuming a mean density of 2.75 Mg/m^3, the maximum burial depth is 35 km. The inset at bottom right in Figure 13 shows the location of samples together with the estimated depth (in kilometers) and temperature at metamorphism. The sample farthest from the Alpine fault, located at the garnet isograd, gives a temperature of 420°C and a pressure of 5.1 kbar equivalent to a depth of 20 km. These rocks, collected over a 5 km wide section, were initially metamorphosed at depths from 20 to 35 km.

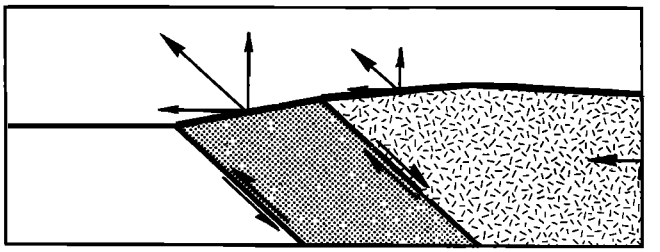

Figure 16. Cartoon of lower crust intrusion in convergent zone showing velocities normal to the plate boundary. Particle velocities (large arrowheads) are relative to the foot wall of the thrust, which is held fixed. Vertical and horizontal components have small arrowheads. On the right the plate convergence component is shown by the horizontal arrow.

3.3.4.2. Ductile deformation in the high-grade schists: *Grapes and Watanabe* [1992] suggest that the thinning of the condensed section to one third of its original thickness occurred during the late Cenozoic by ductile flattening of the schists normal to foliation during their uplift toward the surface. They add that shortening normal to the steeply dipping schistosity could also occur during strike-slip motion resulting from drag along the Alpine fault. Ductilely deformed quartz veins within the high-grade schists [*Holm et al.*, 1989] indicate shortening strains of at least 50% normal to schistosity. They form part of a regionally consistent sequence of structures ranging from the brittle displacements on deglaciated surfaces through structures exhibiting brittle-ductile transitional to ductile behavior.

3.3.4.3. Intrusive body: The 5-km-wide sequence of oligoclase and garnet zone schists along the Alpine fault adjacent to Franz Josef and Fox Glaciers form a steeply dipping tabular body of lower crustal rocks first unroofed about 3 Ma, judging by the earliest appearance of high-grade schist in the Waiho-1 borehole [*Sutherland*, 1996]. At the base of the body is a 1-km-thick sequence of mylonitic rocks and the Alpine fault [*Sibson et al.*, 1979]. This highly condensed metamorphic sequence represents some 15 km of vertical section when the rocks were metamorphosed [*Grapes and Watanabe*, 1992]. The rocks within the sequence contain mesoscopic structures of ductile, brittle-ductile and brittle nature [*Holm et al.*, 1989]. K-Ar and zircon fission track ages are all less than 5 Ma, and it has been argued above that these ages may be overestimates of the time since the rocks cooled through their blocking temperatures. The rocks are all strongly foliated, with the foliation dipping steeply southeast with the bounding faults.

The overall structure of the high-grade metamorphic rocks (strongly foliated, mylonitic near the basal thrust

with intense internal deformation developed during emplacement, young K-Ar and fission track ages, and steep temperature gradients) points to their rapid emplacement directly from the lower crust. The highly condensed section, in the Fox–Franz Josef area at least, points to possible emplacement by a diapiric-like extrusion. If so, then the extruded body would necessarily be fault bounded, in the base by a thrust and at the top by a normal or detachment fault. Such a fault is reported from the valley of the Franz Josef Glacier, on the northeast face of Mount Roon, where biotite schist abuts oligoclase and garnet zone schist across a normal fault or detachment that dips moderately southeast (S. Cox, personal communication, 1996). Whether this fault is currently active and contemporary with the emplacement of the high-grade metamorphic rocks is unknown; it may be much older. The driving force emplacing such an intrusion could be the load of 3 km of topography acting on hot, weak, and effectively fluid material, which when exposed along the low elevations adjacent to the Alpine fault, erodes as fast as it is emplaced.

The speed of emplacement can be deduced from the observation that slip on the Alpine fault is thought to be around 30 mm/yr, and the direction of slip from stretching lineations and transfer faults is about 35° to the fault. At the Alpine fault, therefore, the strike-slip component would be 30 mm/yr, and normal component of velocity would be around 21 mm/yr. The condensed sequence of the schists suggests that they could be transported even faster than the plates, being squeezed out in front of the advancing upper plate like toothpaste.

Similar structural associations characteristic of lower crustal extrusion within continental convergence zones are widespread, an example being the central Himalaya, where ductile, lower crust has been squeezed outward from the collision zone over the advancing foreland [*Burchfiel and Royden*, 1985]. Similar structures are reported elsewhere in the NW Himalaya [*Vince and Treloar*, 1996]. The characteristic structural association is, as here, of high-grade metamorphic rocks forming a tabular body dipping in toward the orogen bounded on the base by a thrust and on the roof by a "normal" or detachment fault. The rocks of the extrusion zone are younger than the enclosing rocks and contain evidence of recent ductile and brittle-ductile deformation overprinted by near-surface brittle deformation. In a sense, this structural association is the equivalent in convergent zones to metamorphic core complexes in extensional zones.

4. DISCUSSION

4.1. Rheological Modeling

General issues of why the South Island plate boundary zone is asymmetric, why major faults occur where they do, how the upper and lower lithosphere separate in the collision, and the likely temperature distribution are addressed by rheological modeling of the collision. *Koons* [1987, 1989, 1990] in particular has demonstrated the importance of erosional, thermal, and rheological parameters in addressing these issues. The two-sided orogen, a development of the model of a critically deforming wedge, is one outcome of the study. *Beaumont et al.* [1996] provide a number of models by which the relative role of deformation and model parameters can be determined. Such geological modeling is a way of investigating input data consistency and inferring details of deformation in an orogen from the physics of deformation, some critical kinematic observations, and knowledge or inference of structural parameters. *Batt and Braun* [1997] develop a thermomechanical evolution of compressional orogens in general, and the Southern Alps in particular, and predict the distribution of apparent ages of isotopic systems. They find good agreement in the case of the Southern Alps using displacement and velocity boundary conditions similar to those given here.

Most modeling has looked only at the convergence of the plate boundary, but *Koons and Henderson* [1995], with a sandbox analogue, and *Koons* [1994], with three-dimensional theoretical models, have examined the consequences of oblique slip. Such modeling has suggested some modes of deformation that are clearly observed, like the "escape tectonics" of the northern segment, where material is transported away from the collision zone to be overthrust, and others, such as basal detachment propagating eastward toward the east coast of the South Island, that are more elusive.

4.2. Kinematic Parameters

The kinematic input in rheological modeling is in several cases deficient. Too much weight has been placed on the rate and pattern of uplift. However, these are poorly known and, indeed, incorrect in many of the fission track studies, while the total amount and present rate of compression are well determined. The amount of shortening is about 100 km across the Southern Alps and Alpine fault and is certainly quite sufficient that uplift and erosion must balance the compression. The issue is not whether they do balance—we just do not know the rates and amount of uplift or of erosion well enough to raise this question. A close balance is decided because within the central segment of the plate boundary there is no alternative process to accommodate the compression. The new kinematic and structural information that will appear over the next few years combined with historical displacement parameters from plate tectonics are needed for rheological modeling to be taken further.

4.3. Earthquakes

No large earthquakes are known to have occurred on the central Alpine fault in the last 170 years, and even on maps of small events the region is clearly anomalous in being a relatively quiet region, a gap, on an otherwise very active plate boundary. *Eberhart-Phillips* [1995], in a 3-year study of relocated events in the vicinity of the

Alpine fault recorded on the New Zealand national seismograph network, identifies nine events per year, in the magnitude range 2.5–3.6. A broad, diffuse zone of low-level seismicity extends southeast away from the fault. Earthquake locations distributed along the full length of the central segment of the plate boundary, projected onto a perpendicular profile, show that the base of the seismogenic zone deepens from 10 km at the fault to more than 20 km, 70 km to the southeast. This study does not distinguish between the central part of the Alpine fault, where there is evidence of high temperatures at shallow depth, and its cooler and presumably more brittle extremities.

The comparative lack of seismicity has raised the question of the long-term likelihood of large events in the near future. Is the plate motion being dissipated by some aseismic process, or is the strain steadily accumulating to eventually release as a great event? Paleoseismic investigations on the southern Alpine fault, near Lake McKerrow, reveal repeated offsets of geological features of around 8–12 m that are reasonably presumed to accompany past earthquakes [*Sutherland and Norris*, 1995]. A few hundred years separate individual offsets, and the last event was ~300–400 years ago. If the whole 450 km of the on-land Alpine fault were to rupture with offsets of this size, an earthquake of very large magnitude indeed would take place. This region, at the northern point of the Fiordland block, is not aseismic on any map: it is one of the most seismic regions in the country, so it is not clear that a rupture there will propagate along the central Alpine fault, where the thermal structure is likely to be very different. In the south the Alpine fault separates the Fiordland block from the west coast, and there has been little differential uplift on either side. Also, the leading edge of the subducted oceanic lithosphere underlies the region and will lead to lower heat flow on the southern segment of the Alpine fault. Elevated temperatures are not expected to occur to anything like the same degree as in the greatly uplifted, high-grade schists of the central Alpine fault. There, with the depth of the ductile-brittle boundary around 6 km, it seems unlikely that the volume of brittle rock could be sufficient to accumulate the elastic energy necessary to generate a great earthquake. How a mixed boundary with a thick, cold, and brittle segment that merges into a thin, hot, and largely ductile segment would behave is unknown.

Nor does the structure of the Alpine fault described by *Norris and Cooper* [1995], with its scalloped, segmented form of short thrusts linked by strike-slip transfer faults (Figure 13, top left inset) suggest periodic rupture by major through going events that involve individual displacements of around 10 m every few hundred years. *Cooper and Norris* [1995] have correctly pointed out the contrast in form and structure of the Alpine fault and its associated mylonites between the areas north and south of Haast River (just to the north of Jackson Bay (Figure 13)). To the south is clear evidence of earthquakes and a sharp and distinct trace; to the north this evidence is lacking (or at least not yet described), and the overall form of the fault does not indicate a major, single, through going rupture.

There are some observations that suggest earthquakes with large offset do occur in the central Alpine fault region. *J. Adams* [1981] identifies an abrupt change in height at the fault of an aggradation surface developed on gravels deposited soon after the retreat of the glaciers at two places north of the Franz Josef region. The lack of displacement where the fault crosses younger, smooth terraces implies that the displacement on the older surface is episodic and perhaps seismic. Radiocarbon dates from the aggraded gravels apparently cluster in groups at ~500-year intervals and suggest offsets of around 5 m every 500 years or so.

We need to establish with much greater confidence the actual kinematics and thermal structure of this boundary before we can determine its likely future seismic behavior.

5. CONCLUSION

The plate boundary through the South Island of New Zealand is an active, young, and well-exposed compressional orogen. As a plate boundary within continental lithosphere it is unusually narrow, and in this it differs from the very broad scale deformation that occurs on many other plate boundaries in continental lithosphere. There are several reasons why this could be so.

1. It is geologically young, with significant compression commencing only 6 Myr ago.

2. The part of the Australian-Pacific plate boundary with continental lithosphere on both sides is only about 500 km long. To the north and south of the South Island the plate boundary involves oceanic lithosphere on at least one side and is typically narrow and clearly defined like oceanic plate boundaries elsewhere. The tightly controlled position of the plate boundary outside the South Island is expected to inhibit the spread of the deformation that might otherwise occur.

3. While the crust east of the Alpine fault is about 30 km thick, it is not typically continental in composition. It consists of a 25-km-thick pile of complexly deformed late Paleozoic and Mesozoic sedimentary rock that has accumulated on Mesozoic ocean floor. It became progressively attached to the margin of Gondwana through subduction of the oceanic lithosphere throughout the Mesozoic that ceased in the mid-Cretaceous. The floor to the sediments and their regionally metamorphosed equivalent is therefore probably Cretaceous oceanic crust that is being subducted today under the Southern Alps.

Recent intensive kinematic and seismic studies will add much to our knowledge of this plate boundary. We can expect to determine the active processes of deformation, including seismicity, to a much greater depth of

understanding than we have at present. This is no academic pursuit; the seismic behavior of the Alpine fault is a matter of concern that affects not only Earth scientists but also substantial communities throughout the South Island of New Zealand. It is the compression resulting from the change in relative motion of the Pacific and Australian plate that elevated most of the land of today above sea level, and it is the continuing motion since then that has molded its shape and created its mountains. Physical New Zealand is the product of forces developed well beyond its shores, and in understanding the processes of its development, we add to our understanding of the Earth itself.

ACKNOWLEDGMENTS. The paper was written while I was Visiting Fellow at Gonville and Caius College, University of Cambridge, and I thank the Master and Fellows of the College for the opportunity of a sabbatical visit. I also thank Dan McKenzie, James Jackson, and Nick McCave, Department of Earth Sciences, University of Cambridge, for making my visit so pleasant and rewarding. I am grateful for critical reviews of an early manuscript by Alan Smith, Duncan Agnew, Kelvin Berryman, Rupert Sutherland, and Rick Allis, which mellowed my views and corrected some errors. Research funding in New Zealand was supported by grants from the Foundation for Research, Science and Technology through PGSF funding and extensive support from Victoria University of Wellington.

Kevin Furlong was the Editor responsible for this paper. He thanks Rick Allis and Rupert Sutherland for technical reviews, and Michael Perfit for his cross-disciplinary review.

REFERENCES

Adams, C. J., Age and origin of the Southern Alps, *Bull. Roy. Soc. N. Z.*, *18*, 73–78, 1979.

Adams, C. J., Uplift rates and thermal structure in the Alpine fault zone and Alpine schists, Southern Alps, New Zealand, *Geol. Soc. Spec. Publ. London*, *9*, 211–222, 1981.

Adams, C. J., and J. E. Gabites, Age of metamorphism and uplift in the Haast Schist Group at Haast Pass, Lake Wanaka and Lake Hawea, South Island, New Zealand, *N. Z. J. Geol. Geophys.*, *28*, 85–96, 1985.

Adams, J., Vertical drag on the Alpine fault, New Zealand, *Bull. R. Soc. N. Z.*, *18*, 47–54, 1979.

Adams, J., Contemporary uplift and erosion of the Southern Alps of New Zealand, *Geol. Soc. Am. Bull., Part 2*, *91*, 1–114, 1980.

Adams, J., Paleoseismicity of the Alpine fault seismic gap, New Zealand, *Geology*, *8*, 72–76, 1981.

Allis, R. G., and Y. Shi, New insights to temperature and pressure beneath the central Southern Alps, New Zealand, *N. Z. J. Geol. Geophys.*, *38*, 585–592, 1995.

Anderson, H., T. Webb, and J. Jackson, Focal mechanisms of large earthquakes in the South Island of New Zealand: Implications for the accommodation of Pacific-Australia plate motion, *Geophys. J. Int.*, *115*, 1032–1054, 1993.

Árnadóttir, T., J. Beavan, and C. Pearson, Deformation associated with the 18 June 1994 Arthur's Pass earthquake, New Zealand, *N. Z. J. Geol. Geophys.*, *38*, 553–558, 1995.

Barnes, P. M., Active folding of Pleistocene unconformities on the edge of the Australian-Pacific plate boundary zone, offshore North Canterbury, New Zealand, *Tectonics*, *15*, 623–640, 1996.

Batt, G. E., and J. Braun, On the thermomechanical evolution of compressional orogens, *Geophys. J. Int.*, *128*, 364–382, 1997.

Beaumont, C., P. J. J. Kamp, J. Hamiliton, and P. Fullsack, The continental collision zone, South Island, New Zealand: Comparison of geodynamical models and observations, *J. Geophys. Res.*, *101*, 3333–3359, 1996.

Berryman, K. R., S. Beanland, A. F. Cooper, H. N. Cutten, R. J. Norris, and P. R. Wood, The Alpine fault, New Zealand: Variation in Quaternary structural style and geomorphic expression, *Ann. Tect.*, *6*, suppl., 126–163, 1992.

Bibby, H. M., Geodetically determined strain across the southern end of the Tonga-Kermadec-Hikurangi subduction zone, *Geophys. J. R. Astron. Soc.*, *66*, 513–533, 1981.

Bull, W. B., and A. F. Cooper, Uplifted marine terraces along the Alpine fault, New Zealand, *Science*, *240*, 804–805, 1986.

Burchfiel, B. C., and L. H. Royden, North-south extension within the convergent Himalyan region, *Geology*, *13*, 679–682, 1985.

Cande, S., and D. V. Kent, A new geomagnetic polarity time scale for the Late Cretaceous and Cenozoic, *J. Geophys. Res.*, *97*, 13,917–13,951, 1992.

Cande, S. C., and D. V. Kent, Revised geomagnetic polarity timescale, *J. Geophys. Res.*, *100*, 6093–6095, 1995.

Cande, S. C., C. A. Raymond, J. Stock, and W. F. Haxby, Geophysics of the Pitman Fracture Zone and Pacific-Antarctic plate motions during the Cenozoic, *Science*, *270*, 947–953, 1995.

Carter, L., and I. N. McCave, Development of sediment drifts approaching an active plate margin under the SW Pacific deep western boundary current, *Paleoceanography*, *9*, 1061–1085, 1994.

Carter, L., K. B. Lewis, and F. J. Davey, Faults in Cook Strait and their bearing on the structure of central New Zealand, *N. Z. J. Geol. Geophys.*, *31*, 431–446, 1988.

Chase, C. G., Plate kinematics: The Americas, East Africa and the rest of the world, *Earth Planet. Sci. Lett.*, *37*, 353–368, 1978.

Christoffel, D. A., and W. J. M. van der Linden, Macquarie Ridge–New Zealand Alpine fault transition, in *Antarctic Oceanology II: The Australian–New Zealand Sector*, *Antarct. Res. Ser.*, vol. 19, edited by D. E. Hayes, pp. 235–242, AGU, Washington, D. C., 1972.

Cooper, A. F., and D. G. Bishop, Uplift rates and high level marine platforms associated with the Alpine faut at Okura River, South Westland, *Bull. R. Soc. N. Z.*, *18*, 35–43, 1979.

Cooper, A. F., and R. J. Norris, Displacement on the Alpine fault at Haast River, South Westland, New Zealand, *N. Z. J. Geol. Geophys.*, *38*, 509–514, 1995.

Cowan, H. A., Late Quaternary displacements on the Hope fault at Glynn Wye, North Canterbury, *N. Z. J. Geol. Geophys.*, *33*, 285–293, 1990.

Davey, F. J., and E. G. C. Smith, The tectonic setting of the Fiordland region, south-west New Zealand, *Geophys. J. R. Astron. Soc.*, *72*, 23–38, 1983.

DeMets, C., R. G. Gordon, D. F. Argus, and S. Stein, Current plate motions, *Geophys. J. Int.*, *101*, 425–478, 1990.

DeMets, C., R. G. Gordon, D. F. Argus, and S. Stein, Effect of recent revisions to the geomagnetic time scale on estimates of current plate motions, *Geophys. Res. Lett.*, *21*, 2191–2194, 1994.

Eberhart-Phillips, D., Examination of seismicity in the central Alpine fault region, South Island, New Zealand, *N. Z. J. Geol. Geophys.*, *38*, 571–578, 1995.

Gage, M., The Greymouth Coalfield, *Bull. Geol. Survey N. Z.*, *45*, 68–71, 1952.

Grapes, R. H., Uplift and exhumation of Alpine schist, Southern Alps, *N. Z. J. Geol. Geophys.*, *38*, 525–533, 1995.

Grapes, R., and T. Watanabe, Metamorphism and uplift of Alpine schist in the Franz Josef–Fox Glacier area of the Southern Alps, New Zealand, *J. Metamorph. Geol.*, *10*, 171–180, 1992.

Haines, A. J., Calculating velocity fields across plate boundaries from observed shear rates, *Geophys. J. R. Astron. Soc.*, *68*, 203–209, 1982.

Haxby, W. F., Gravity field of the World's Oceans, map, NOAA Natl. Geophys. Data Cent., Boulder, Colo., 1987.

Holm, D. K., R. J. Norris, and D. Craw, Brittle/ductile deformation in a zone of rapid uplift: Central Southern Alps, New Zealand, *Tectonics*, *8*, 153–168, 1989.

Holt, W. E., and H. J. Haines, The kinematics of northern South Island, New Zealand, determined from geologic strain rates, *J. Geophys. Res.*, *100*, 17,991–18,010, 1995.

Hurford, A. J., Cooling and uplift patterns in the Lepontine Alps, south central Switzerland, and an age of vertical movement on the Insubric fault line, *Contrib. Mineral. Petrol.*, *92*, 413–427, 1988.

Jenkins, G. R. T., D. Craw, and A. E. Fallick, Stable isotopic and fluid inclusion evidence for meteoric fluid penetration into an active mountain belt; Alpine schist, New Zealand, *J. Metamorph. Geol.*, *12*, 429–444, 1994.

Kamp, P. J. J., and J. M. Tippett, Dynamics of Pacific plate crust in the South Island (New Zealand) zone of oblique continent-continent convergence, *J. Geophys. Res.*, *98*, 16,105–16,118, 1993.

Kamp, P. J. J., P. F. Green, and S. H. White, Fission track analysis reveals character of collisional tectonics in New Zealand, *Tectonics*, *8*, 169–195, 1989.

Kamp, P. J. J., P. F. Green, and J. M. Tippett, Tectonic architecture of the mountain front-foreland basin transition, South Island, New Zealand, assessed by fission-track analysis, *Tectonics*, *11*, 98–113, 1992.

Koons, P. O., Some thermal and mechanical consequences of rapid uplift: An example from the Southern Alps, New Zealand, *Earth Planet Sci. Lett.*, *86*, 307–319, 1987.

Koons, P. O., The topographic evolution of collisional mountain belts: A numerical look at the Southern Alps, New Zealand, *Am. J. Sci.*, *289*, 1041–1069, 1989.

Koons, P. O., Two-sided orogen: Collision and erosion from the sandbox to the Southern Alps of New Zealand, *Geology*, *18*, 679–682, 1990.

Koons, P. O., Three-dimensional critical wedges: Tectonics and topography in oblique collisional orogens, *J. Geophys. Res.*, *99*, 12,301–12,315, 1994.

Koons, P. O., and C. M. Henderson, Geodetic analysis of model oblique collision and comparison to the Southern Alps of New Zealand, *N. Z. J. Geol. Geophys.*, *38*, 545–552, 1995.

Lamb, S., and H. M. Bibby, The last 25 Ma of rotational deformation in part of the New Zealand plate boundary zone, *J. Struct. Geol.*, *11*, 473–492, 1989.

Larson, K. M., and J. Freymueller, Relative motions of the Australian, Pacific and Antarctic plates estimated by the Global Positioning System, *Geophys. Res. Lett.*, *22*, 37–40, 1995.

Larson, K. M., J. Freymueller, and S. Phillipsen, Global plate velocities from the Global Positioning System, *J. Geophys. Res.*, *102*, 9961–9981, 1997.

Le Pichon, X., J. Francheteau, and J. Bonnin, *Plate Tectonics*, Elsevier, New York, 1973.

Little, T. A., and A. P. Roberts, Distribution and mechanisms of Neogene to present-day vertical axis rotations, Pacific-Australian plate boundary zone, South Island, New Zealand, *J. Geophys. Res.*, *102*, 20,447–20,468, 1997.

Mason, B., Metamorphism in the Southern Alps of New Zealand, *Bull. Am. Mus. Nat. Hist.*, *123*, 217–248, 1962.

Molnar, P., and P. England, Late Cenozoic uplift of mountain ranges and global climate change: Chicken or egg?, *Nature*, *346*, 29–34, 1990.

Mortimer, N., 1993. Metamorphic zones, terranes, and Cenozoic faulting in the Marlborough Schist, *N. Z. J. Geol. Geophys.*, *36*, 357–368, 1993.

Nathan, S., Upper Cenozoic stratigraphy of south Westland, New Zealand, *N. Z. J. Geol. Geophys.*, *21*, 329–361, 1978.

Nathan, S., H. J. Anderson, R. A. Cook, R. H. Herzer, R. H. Hoskins, J. I. Raine, and D. Smale, Cretaceous and Cenozoic sedimentary basins of the west coast regions, South Island, New Zealand, *N. Z. Geol. Surv. Basin Stud.*, *1*, 1986.

Norris, R. J., and A. F. Cooper, Small-scale fractures, glaciated surface, and recent strain adjacent to the Alpine fault, New Zealand, *Geology*, *14*, 687–690, 1986.

Norris, R. J., and A. F. Cooper, Origin of small-scale segmentation and transpressional thrusting along the Alpine fault, New Zealand, *Bull. Geol. Soc. Am.*, *107*, 231–240, 1995.

Norris, R. J., and I. M. Turnbull, Cenozoic basins adjacent to an evolving transform plate boundary, southwest New Zealand, in *South Pacific Sedimentary Basins*, edited by P. Ballance, pp. 251–270, Elsevier, New York, 1993.

Norris, R. J., R. M. Carter, and I. M. Turnbull, Cainozoic sedimentation in basins adjacent to a major continental transform boundary in southern New Zealand, *J. Geol. Soc. London*, *135*, 191–205, 1978.

Norris, R. J., P. O. Koons, and A. F. Cooper, The obliquely convergent plate boundary in the South Island of New Zealand: Implications for ancient collision zones, *J. Struct. Geol.*, *12*, 715–725, 1990.

Pearson, C., Strain measurements in the northern Waiau Basin, *N. Z. J. Geol. Geophys.*, *35*, 375–379, 1992.

Rait, G., F. Charnier, and D. W. Waters, Landward and seaward directed thrusting accompanying the onset of subduction beneath New Zealand, *Geology*, *19*, 230–233, 1991.

Rattenbury, M. S., Late low-angle thrusting and the Alpine fault, central Westland, New Zealand, *N. Z. J. Geol. Geophys.*, *29*, 437–446, 1986.

Rattenbury, M. S., Timing of mylonitisation west of the Alpine fault, central Westland, New Zealand, *N. Z. J. Geol. Geophys.*, *30*, 287–297, 1987.

Reilly, W. I., Horizontal crustal deformation on the Hikurangi margin, *N. Z. J. Geol. Geophys.*, *33*, 393–400, 1990.

Reyners, M., Subcrustal earthquakes in the central South Island, New Zealand, and the root of Southern Alps, *Geology*, *15*, 1168–1171, 1993.

Reyners, M., and H. Cowan, The transition from subduction to continental collision: Crustal structure in the north Canterbury region, New Zealand, *Geophys. J. Int.*, *115*, 1124–1136, 1993.

Roberts, A. P., Paleomagnetic constraints on the tectonic rotation of the southern Hikurangi margin, New Zealand, *N. Z. J. Geol. Geophys.*, *35*, 311–323, 1992.

Roberts, A. P., Tectonic rotation about the termination of a major strike-slip fault, Marlborough fault system, *Geophys. Res. Lett.*, *22*, 187–190, 1995.

Robinson, R., T. Árnadóttir, J. Beavan, J. Cousins, M. Reyners, R. Van Dissen, T. Webb, and C. Pearson, The M_w 6.7 Arthur's Pass earthquake in the Southern Alps, New Zealand, June 18, 1994, *Seismol. Res. Lett.*, *66*, 11–13, 1995.

Royer, J.-Y., and D. T. Sandwell, Evolution of the Indian Ocean since the Late Cretaceous: Constraints from Geosat altimetry, *J. Geophys. Res.*, *94*, 13,755–13,782, 1989.

Sandwell, D. T., and A. H. F. Smith, Marine gravity anomalies from satellite altimetry, map, Scripps Inst. of Oceanogr., La Jolla, Calif., 1995.

Sheppard, D. S., C. J. Adams, and G. W. Bird, Age of meta-

morphism and uplift of the Alpine schist belt, New Zealand, *Geol. Soc. Am. Bull.*, *86*, 1147–1153, 1975.

Shi, Y., R. Allis, and F. Davey, Thermal modelling of the Southern Alps, *Pure Appl. Geophys.*, *146*, 469–501, 1996.

Sibson, R. H., S. H. White, and B. K. Atkinson, Fault rock distribution and structure within the Alpine fault zone: A preliminary account, *Bull. Roy. Soc. N. Z.*, *18*, 55–65, 1979.

Stern, T. A., Gravity anomalies and crustal loading at and adjacent to the Alpine fault, New Zealand, *N. Z. J. Geol. Geophys.*, *38*, 593–600, 1995.

Stock, J., and P. Molnar, Revised history of early Tertiary plate motion in the southwest Pacific, *Nature*, *325*, 495–499, 1987.

Suggate, R. P., The Alpine fault, *Trans. R. Soc. N. Z.*, *2*, 105–129, 1963.

Sutherland, R., Displacement since the Pliocene along the southern section of the Alpine fault, New Zealand, *Geology*, *22*, 327–330, 1994.

Sutherland, R., The Australian-Pacific boundary and Cenozoic plate motions in the SW Pacific: Some constraints from Geosat data, *Tectonics*, *14*, 819–831, 1995.

Sutherland, R., Transpressional development of the Australia-Pacific boundary through southern South Island, New Zealand: Constraints from Miocene-Pliocene sediments, Waiho-1 borehole, south Westland, *N. Z. J. Geol. Geophys.*, *39*, 251–264, 1996.

Sutherland, R., and R. J. Norris, Late Quaternary displacement rate, paleoseismicity, and geomorphic evolution of the Alpine fault: Evidence from Hokuri Creek, south Westland, New Zealand, *N. Z. J. Geol. Geophys.*, *38*, 419–430, 1995.

Sutherland, R., S. Nathan, and I. M. Turnbull, Pliocene-Quaternary sedimentation and Alpine fault related tectonics in the lower Cascade Valley, south Westland, New Zealand, *N. Z. J. Geol. Geophys.*, *38*, 431–450, 1995.

Tagami, T., A. Carter, and A. J. Hurford, Natural long-term annealing of the zircon fission-track system in Vienna Basin deep borehole samples: Constraints on the partial annealing zone and closure temperature, *Chem. Geol.*, *130*, 147–157, 1996.

Tippett, J. M., and P. J. J. Kamp, Fission track analysis of the late Cenozoic vertical kinematics of continental Pacific crust, South Island, New Zealand, *J. Geophys. Res.*, *98*, 16,119–16,148, 1993a.

Tippett, J. M., and P. J. J. Kamp, The role of faulting in rock uplift in the Southern Alps, New Zealand, *N. Z. J. Geol. Geophys.*, *36*, 497–504, 1993b.

Van Dissen, R., and R. S. Yeats, Hope fault, Jordan thrust and uplift of the seaward Kaikoura range, *Geology*, *19*, 393–396, 1991.

Vickery, S., and S. Lamb, Large tectonic rotations since the early Miocene in a convergent plate-boundary zone, South Island, New Zealand, *Earth Planet. Sci. Lett.*, *136*, 43–59, 1995.

Vince, K. J., and P. J. Treloar, Miocene, north-vergent extensional displacements along the main mantle thrust, N.W. Himalaya, Pakistan, *J. Geol. Soc. London*, *153*, 677–680, 1996.

Walcott, R. I., Present tectonics and Late Cenozoic evolution of New Zealand, *Geophys. J. R. Astron. Soc.*, *52*, 137–164, 1978.

Walcott, R. I., The kinematics of the plate boundary zone through New Zealand: A comparison of short- and long-term deformations, *Geophys. J. R. Astron. Soc.*, *79*, 613–633, 1984.

Walcott, R. I., D. A. Christoffel, and T. C. Mumme, Bending within the axial tectonic belt of New Zealand in the last 9 Myr from paleomagnetic data, *Earth Planet. Sci. Lett.*, *52*, 427–434, 1981.

Ward, C. M., Marine terraces of the Waitutu district and their relation to the late Cenozoic tectonics of the southern Fiordland region, New Zealand, *J. R. Soc. N. Z.*, *18*, 1–28, 1988.

Wellman, H. W., An uplift map for the South Island of New Zealand, and a model for the uplift of the Southern Alps, *Bull. R. Soc. N. Z.*, *18*, 13–20, 1979.

Wellman, H. W., and A. T. Wilson, Notes on the geology and archaeology of the Martins Bay district, *N. Z. J. Geol. Geophys.*, *7*, 702–721, 1964.

White, S. H., and P. F. Green, Tectonic development of the Alpine fault zone, New Zealand: A fission track study, *Geology*, *14*, 124–127, 1986.

Wood, R. A., Structure and seismic stratigraphy of the western Challenger Plateau, *N. Z. Geol. Geophys.*, *34*, 1–9, 1991.

Yamada, R., T. Tagami, S. Nishimura, and H. Ito, Annealing kinetics of fission tracks in zircon: An experimental study, *Chem. Geol.*, *122*, 249–258, 1995.

Yeats, R. S., Tectonic map of central Otago based on satellite imagery, *N. Z. J. Geol. Geophys.*, *30*, 261–271, 1987.

R. I. Walcott, School of Earth Sciences, Victoria University of Wellington, Wellington, New Zealand. (e-mail: walcott@rses.vuw.ac.nz)